1979

A polarographic study of Fe(II) and Fe(III) complexes with catechol

Wen-Tang Shen
Portland State University

AN ABSTRACT OF THE THESIS OF Wen-Tang Shen for the Master of Science in Chemistry presented November 29, 1979.

Title: A Polarographic Study of Fe(II) and Fe(III) Complexes with Catechol.

APPROVED BY MEMBERS OF THE THESIS COMMITTEE:

Dennis W. Barnum, Chairman

Morris B. Silverman

David W. McClure

A study of the anodic polarography of catechol in 0.100 F sodium perchlorate is presented. A new wave is observed in alkaline solutions which is different from the simple oxidation wave of catechol to ortho-quinone observed by previous workers. The importance of buffer materials is discussed and a possible explanation of the new wave is suggested.

A study of the polarography behavior of Fe(II) and Fe(III) in the presence of catechol is reported. In the case of reduction of Fe(III) in the presence of catechol, two steps occur at about -1.5 and -1.8 volts (vs. SCE) at pH higher than 11.6 corresponding

to one electron reduction of Fe(III) to Fe(II) and successive two electron reduction of Fe(II) to Fe(s). At lower pH these two steps are too close together to be resolved. An oxidation wave and a reduction wave are recorded for the electrolysis of Fe(II) in the presence of catechol: the oxidation wave is observed between pH 7 and 12.3. The curve showing dependence of the limiting current on pH is similar to the distribution curve of Fe(cat). It is therefore suggested that only Fe(cat) is oxidized and observed here. The reduction wave of Fe(II) in the presence of catechol is irreversible and shifted from -1.5 to -1.8 volts upon complex formation. A calculation of formation constants, β_1 and β_2, was achieved according to an equation which relates the shifts of half-wave potential to the formation constants. Using parentheses to indicate activities, the results are:

$$\beta_1 = 7 \times 10^7 = \frac{(Fe(cat))}{(Fe^{2+})(cat^{2-})}$$

and

$$\beta_2 = 4 \times 10^{12} = \frac{(Fe(cat)_2^{2-})}{(Fe^{2+})(cat^{2-})^2}$$

at T = 25°C, and ionic strength = 0.100($NaClO_4$).

A POLAROGRAPHIC STUDY OF Fe (II) AND Fe (III) COMPLEXES WITH CATECHOL

by

WEN-TANG SHEN

A thesis submitted in partial fulfillment of the requirements for the degree of

MASTER OF SCIENCE
in
CHEMISTRY

Portland State University
1979

TO THE OFFICE OF GRADUATE STUDIES AND RESEARCH:

The members of the Committee approve the thesis of Wen-Tang Shen presented November 29, 1979.

[redacted]

Dennis W. Barnum, Chairman

[redacted]

Morris B. Silverman

[redacted]

David W. McClure

APPROVED:

[redacted]

David W. McClure, Chairman, Department of Chemistry

[redacted]

Stanley E. Rauch, Dean of Graduate Studies and Research

ACKNOWLEDGMENTS

My sincere appreciation is expressed to Dr. D.W. Barnum for his helpful discussion in the course of this research. A generous gift of triple distilled mercury from Dr. D.K. Roe and assistance in typing this thesis by A. McFarlane and W. Chambers are acknowledged with thanks. Appreciation is also due to Ahmad Mehrabzadeh, Dianne Hunter, Mario Aparicio-Razo, Michael Fleming and Yat-Sang Fanjung for their advice and counsel. Special thanks are expressed to my wife, Wai-Hing Shen, for her constant encouragement and understanding.

TABLE OF CONTENTS

PAGE

LIST OF TABLES

LIST OF FIGURES

FIGURE PAGE

CHAPTER I

THE POLAROGRAPHY OF CATECHOL

INTRODUCTION

Molecules containing the aromatic vic-diol group, such as catechol, are of widespread biological occurrence and importance. Many are found in by-products of the metabolism of plants and animals; several are of pharmacological use in such diverse areas as the treatment of hypertension, Parkinson's disease, breast cancer, etc. Recently the significance of catechol chemistry has gained recognition among coordination chemists,[1-3] synthetic organic chemists,[4] enzymologists,[5,6] and water pollution scientists.[7,8] Investigations include auto-oxidation of catechol in the absence of catalyst,[9] metal catalyzed oxidation,[10,11] the metal chelate catalyzed oxidation of catechols,[12] and enzymatic oxidation of catechol. Several techniques have been used such as spectrophotometry, cyclic voltammetry, polarography, and nuclear magnetic resonance spectroscopy.

Several workers have observed a polarographic wave at the dropping mercury electrode due to oxidation of catechol to ortho-quinone*.

$$H_2cat \rightleftharpoons qn + 2H^+ + 2e^- \qquad (1)$$

*The following abbreviations will be used throughout this thesis:
H_2cat = catechol
$Hcat^-$ = mono-protonated anion of catechol
cat^{2-} = catechol anion
qn = ortho-quinone

However, there is no data on the effect of pH on i_{lim}, the effect of mercury column height, and there is conflicting information about the reversibility. Furthermore, in preliminary experiments done in the present work the expected wave was not observed. In view of the incomplete and conflicting information a polarographic study of catechol was carried out.

EXPERIMENTAL

Materials

Sodium hydroxide (J.T. Baker), perchloric acid, potassium chloride, potassium nitrate (Mallinckrodt) and dipotassium hydrogen phosphate (Baker and Adamson) were of analytical reagent grade and were used without further purification. Catechol (Matheson, Coleman and Bell) was purified by vacuum distillation.

Sodium perchlorate, 0.100 F, was preprepared by neutralizing a known volume of standard 0.6 F perchloric acid with carbonate free sodium hydroxide and diluting to 1.000 liter. This stock 0.6 F perchloric acid solution was standardized against sodium carbonate using bromocresol green as indicator. The final concentration of 0.100 F sodium perchlorate was calculated from the volume and the concentration of stock perchloric acid solution.

Mercury was purified by treatment with 10% nitric acid.

Triton X-100 (J.T. Baker) was chosen as maximum suppressor.

Apparatus

The electrolytic cell, was a 250-ml "tall form" beaker arranged as shown in Fig. 1. It was so constructed that the following functions can be achieved: admission of nitrogen, removal of dissolved oxygen, pH measurement and addition of acid or base for pH adjustment. A J-type salt bridge was used to connect the dropping mercury electrode to a saturated calomel electrode. The potential of the SCE reference electrode

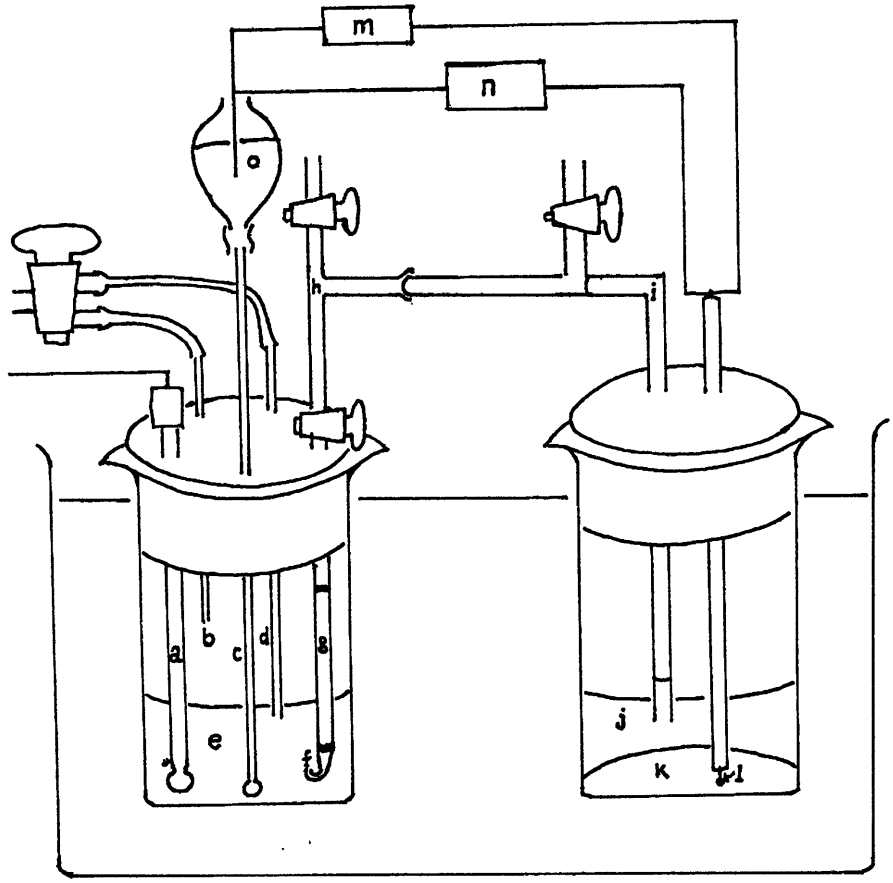

Figure 1. Apparatus for polarographic work.

a) combination glass electrode for pH measurement
b) nitrogen inlet
c) dropping mercury electrode
d) nitrogen inlet
e) test solution
f) J-type bridge tip filled with 0.100F sodium perchlorate
g) 3% agar in saturated potassium chloride
h) saturated calomel solution
i) 3% agar in saturated potassium chloride
j) saturated calomel solution
k) mercury pool
l) platinum contact
m) Sargent polarograph, Model XV
n) Tektronix DM-502 voltmeter
o) mercury reservoir

was checked and confirmed by comparing it with a commercial calomel electrode and a commercial silver/silver chloride electrode.

All experiments were performed in a thermostated water bath at 25°C. The capillary constant was determined for 0.100 F sodium perchlorate supporting electrolyte with various potentials applied across the terminals of a conventional H-type cell. These data are summarized in TABLE I and variation of drop time with applied voltage is plotted in Fig. 2.

TABLE I

CAPILLARY CONSTANT DETERMINED FOR
0.100 F SODIUM PERCHLORATE

Applied Potential, V vs. SCE	drop time* (sec/drop) t	mercury** weight (mg/drop)	Hg flow rate*** (mg/sec) m	$\frac{2}{3}\frac{1}{6}$ $m^{3}t^{6}$
+0.200	3.663	7.578	2.069	2.016
0.000	4.000	8.237	2.059	2.039
-0.200	4.180	8.598	2.057	2.053
-0.400	4.220	8.627	2.044	2.047
-0.600	4.313	8.868	2.056	2.063
-0.800	4.230	8.628	2.040	2.046
-1.000	4.075	8.373	2.055	2.043
-1.200	3.850	8.033	2.086	2.044
-1.400	3.530	7.285	2.064	2.000
-1.600	3.145	6.502	2.067	1.964
-1.800	2.738	5.669	2.070	1.921
-1.925	2.413	4.963	2.057	1.873

*The drop time was recorded for 60 drops and the mean value is reported.

**The mercury weight was measured for 60 drops and the mean value is recorded.

***The flow rate of mercury was calculated from the drop weight and drop time.

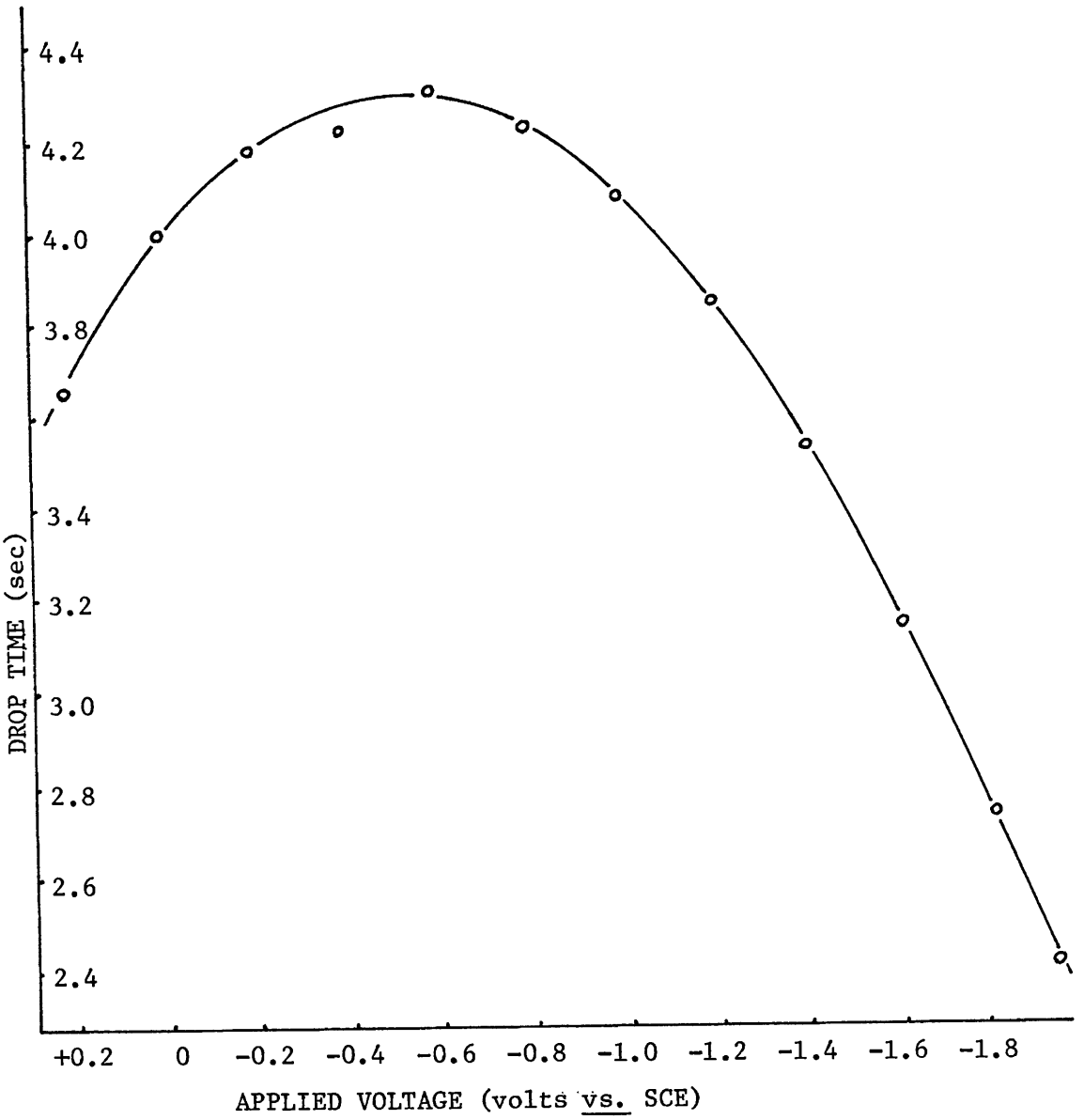

Figure 2. Variation of drop time, t, in 0.100 F $NaClO_4$ as a function of applied voltage, E.

Instrumentation

A Corning Model 12 "expanded scale" pH meter was used to record pH values. Two primary standards were chosen for pH calibration. They were potassium acid phthalate with a pH(S) value of 4.008 and 0.025 F dipotassium hydrogen phosphate - 0.025 F disodium hydrogen phosphate with a pH(S) value of 6.865.

A Sargent Model XV polarograph was used to record polarograms. The applied voltage was accurately read by means of a Tektronix DM-502 digital voltmeter.

Cell resistances for the purpose of IR correction were measured with a Y.S.I. Model 31 conductivity bridge.

Preparation of Catechol Solutions

Special care was taken to exclude air, especially at pH values above 8 where oxidation of catechol occurs rapidly. Water and 0.100 F sodium perchlorate were deoxygenated by bubbling nitrogen through the solution for about 30 minutes before use. Catechol solutions were then prepared and transferred to the electrolysis cell under nitrogen. Finally, the pH was adjusted to the desired value by adding small amounts of 18 F NaOH with a 10 microliter syringe and polarograms were recorded.

RESULTS AND DISCUSSION

Reversibility of the Polarographic Wave for Catechol

Wheeler and Vigneault[16] and Howden and Reynolds[29] plotted E for the oxidation of catechol against log $\{(i_d - i)/i\}$. Such a plot should give a straight line with slope equal to $0.059/n\alpha$, where n is the number of electrons involved in the electrode reaction and α is the electron transfer coefficient. For a reversible electrode reaction $\alpha = 1$, whereas $\alpha < 1$ for irreversible reactions.

As n = 2 in Eq. 1, Wheeler and Vigneault[16] found values of $n\alpha$ from 1.0 to 1.3 and concluded that the wave is irreversible. Actually, such a plot is not a reliable test for reversibility[32]. It is most likely to fail when semi-quinones are produced as intermediates in the electrode reaction, which is exactly the case in the oxidation of catechol.

As discussed in the following section, the half-wave potential at which oxidation occurs at a dropping mercury electrode was found[15,16] in good agreement with the voltage calculated from the Nernst equation. This is good evidence for reversibility. Furthermore, Doskocil[17] prepared aqueous solutions of o-quinone by oxidizing catechol with cerium(IV). He observed a wave for reduction of o-quinone at the same voltage as the oxidation of catechol and noticed that a solution containing both o-quinone and catechol show a single wave that is partly anodic and partly cathodic. Thus, the wave is most certainly reversible.

A New Anodic Wave in Aqueous Catechol Solutions

It would seem that the affect of pH on the half-wave potential is well established from the work of previous investigators. However, quite different results were obtained in the sodium perchlorate solutions used in the present work.

Because the oxidation of catechol to o-quinone is reversible, the half-wave potential should be closely approximated by the Nernst equation:

$$E = 0.816 - \frac{0.0591}{2} \log \frac{(H_2cat)}{(qn)(H^+)^2} - E_{SCE} \qquad (2)$$

where the standard half-cell potential, 0.816 volt, is taken from the potentiometric measurements of Ball and Chien.[33] For the polarographic half-wave potential Eq. 2 gives:

$$E_{\frac{1}{2}} \text{ (vs. SCE)} = 0.57 - 0.059 \text{ pH} \qquad (3)$$

which is almost identical to the equation found by Vlcek.[15] However, Vlcek's equation refers $E_{\frac{1}{2}}$ to a "n-Mercurosulfatelektrode." In the pH region between 9.2 and 13 the principal species of catechol is the $Hcat^-$ ion and the half-cell reaction is

$$Hcat^- = qn + H^+ + 2e^- \qquad (4)$$

Above pH 13, the electrode reaction is

$$cat^= = qn + 2e^- \qquad (5)$$

Combining these equations for the different pH regions gives the dashed line in Fig. 3 for the relationship between the polarographic half-wave potential and pH.

In Fig. 3 data obtained by Wheeler and Vigneault[16] and Howden and Reynolds[29] in buffered solutions are compared with the predicted values. It will be seen that good agreement is obtained over a broad pH range.

However, in the present work in unbuffered sodium perchlorate solutions no anodic wave could be detected below pH 8. Above pH 8 a new wave appears which is different from the wave for the oxidation of catechol. This new wave is shown in Fig. 4.

After correction for residual current and iR drop, the wave equation can be expressed:

$$E = E_{\frac{1}{2}} + \frac{0.059}{n\alpha} \log \{(i_d - i)/i\} \qquad (6)$$

in which E is the applied potential, i is the current and $E_{\frac{1}{2}}$ is the half-wave potential at which current i is equal to half of the diffusion current, i_d. The values of $E_{\frac{1}{2}}$ and $\frac{.059}{n\alpha}$ are reported in TABLE II.

It will be seen that the values of $n\alpha$ are close to 1, but having no knowledge of the degree of reversibility of the new wave (i.e., no knowledge of α) one cannot decide the number of electrons exchanged.

TABLE II

OXIDATION OF 9.73×10^{-3} F CATECHOL IN 0.100 F SODIUM PERCHLORATE AT A DROPPING MERCURY ELECTRODE

pH	i_d obs x 10^6 amp. at E_d	E_d^* vs SCE (in volts)	$E_{\frac{1}{2}}$ vs SCE (in volts)	$\frac{.059}{n\alpha}$** (in volts)
7.37	0.26	+0.10	+0.046	0.071
8.23	1.95	+0.15	+0.034	0.061
9.27	11.40	+0.17	+0.015	0.058
10.25	29.40	+0.30	-0.009	0.078
10.62	29.68	+0.30	-0.025	0.075
11.22	32.96	+0.40	-0.046	0.081

*E_d = potential at which i_d was measured **See Eq. 6

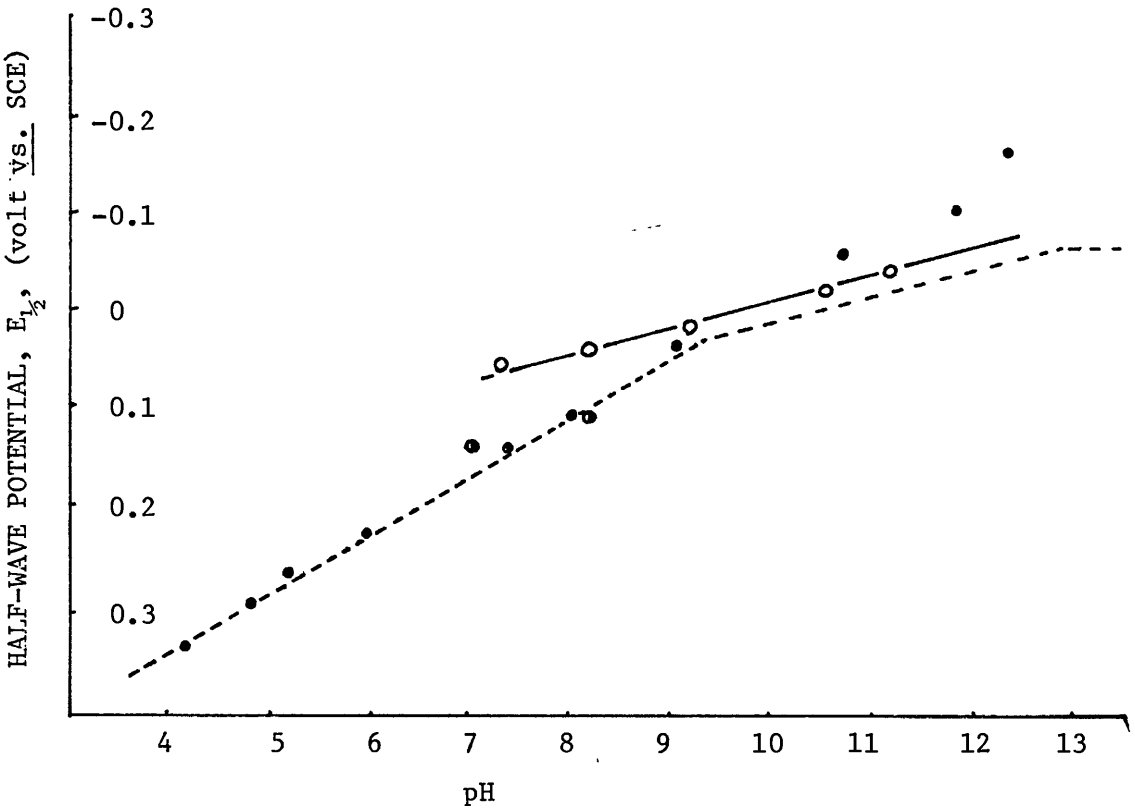

Figure 3. pH influence on half-wave potential of catechol anodic wave.

○ from present work in unbuffered sodium perchlorate.

● from Wheeler and Vigneault (in acetate buffer at pH≤6, in phosphate buffer at 6<pH<9, in glycine buffer at pH pH≥9).

◐ from Howden and Reynolds in phosphate buffer

– – – theoretical curve according to Nernst equation.

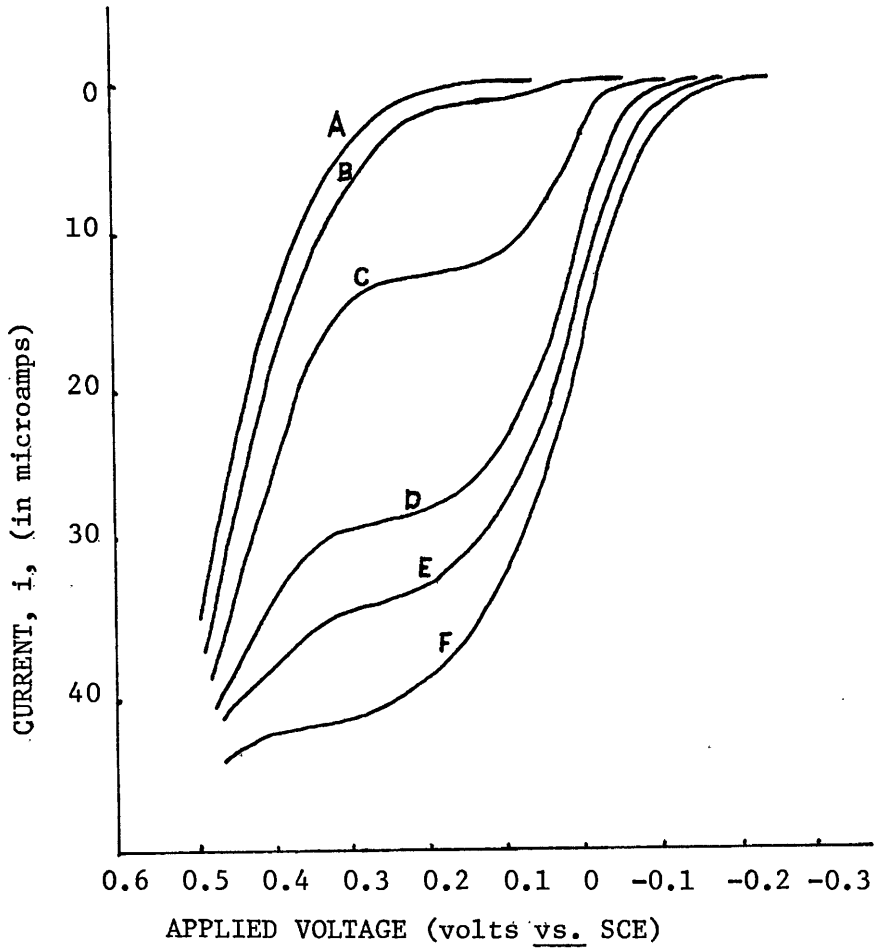

Figure 4. Current-voltage curve of 9.7×10^{-3}F catechol (unbuffered) in 0.1 F sodium perchlorate at the following pH values: A) 7.37 B) 8.23 C) 9.27 D) 10.25 E) 10.62 F) 11.21.

It will be seen in Fig. 4 that the height of the new wave increases with increasing pH. These data are plotted in Fig. 5. This behavior is quite different from that observed for the oxidation of catechol, where the limiting current is diffusion controlled and independent of pH as found by Wheeler and Vigneault.[16] Furthermore, as seen in Fig. 3, the dependence of the half-wave potential on pH is different for the oxidation of catechol and for the new wave.

Because the oxidation of catechol produces acid, one might expect that in the unbuffered perchlorate solutions the pH at the electrode surface will be slightly lower than in the bulk of the solution and the half-wave potential might therefore be shifted to a somewhat more positive voltage. However, this cannot account for the difference in behavior of the two waves with respect to pH because the curve for the new wave actually crosses that for the oxidation of catechol at pH ≈ 10.

Several experiments and tests were carried out to determine that the differences observed between this work and previous work are real:

A) Purity of Catechol. Other workers used commercially available catechol without purification. The catechol used in this work was vacuum distilled. The experiment was repeated using "practical" grade catechol obtained from Matheson, Coleman & Bell. No difference was observed.

B) Purity of Mercury. The mercury used in this work was originally purified by treatment with 10% nitric acid. No difference was observed when it was replaced with distilled mercury.

C) Oxygen. Vlcek made no attempt to remove dissolved oxygen, whereas this work was done with careful exclusion of oxygen. When repeated in the presence of oxygen no change was observed.

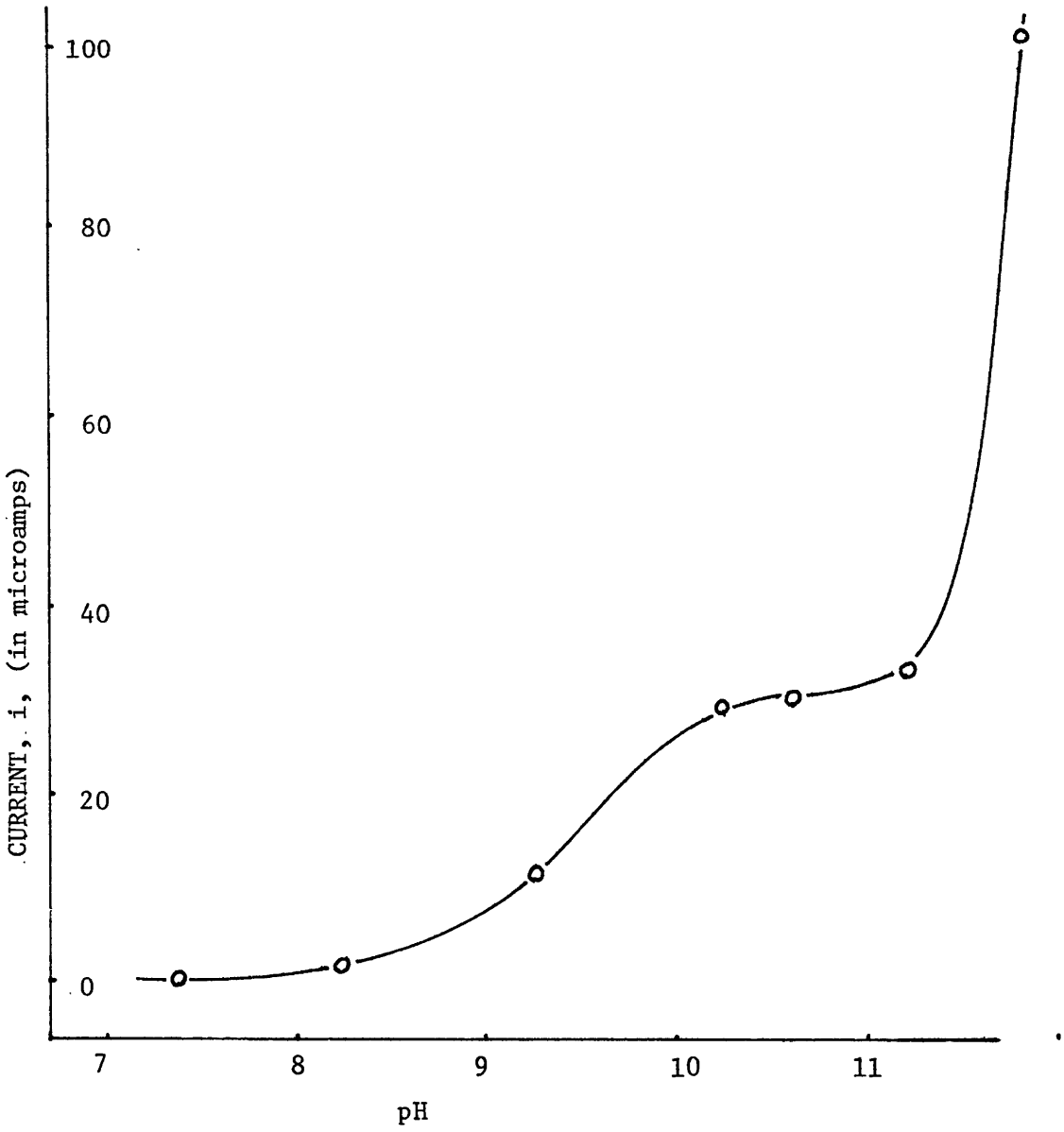

Figure 5. The influence of pH on the limiting current of the anodic wave of catechol observed in this work in unbuffered sodium perchlorate solutions.

D) Light. Repeating the preparation of the catechol solution and measuring the polarogram in a nearly dark room gave no change.

E) Potential of reference electrode. The potential of the reference electrode was checked, and confirmed, by comparing it with a commercial calomel electrode and a commercial silver/silver chloride electrode.

F) Polarograph. To ensure that the polarograph and cell were operating properly polarograms taken with the Sargent Model XV were compared with those measured with a PAR model 174A. No difference was observed.

G) Buffer and supporting electrolyte. In phosphate buffer at pH 6.85 the anodic wave was observed at 0.16 volt. Eq. 6 predicts 0.17 volt, which is good agreement. Addition of sodium perchlorate to the solution did not eliminate the wave. On the other hand, when a solution of catechol in 0.100 F sodium perchlorate was prepared no anodic wave was observed until phosphate was added. Apparently phosphate is required for the electrolytic oxidation of catechol.

Wheeler and Vigneault[16] report $E_{\frac{1}{2}}$ values measured in a glycine buffer. It was found in this work that glycine itself gives an anodic wave in the same region and no difference could be distinguished between solutions containing catechol and those without catechol.

A possible explanation for the new wave is that it is due to oxidation of metallic mercury to form a mercury-catechol complex. Perhaps:

$$Hg^{\circ} + Hcat^{-} \rightleftharpoons Hg(cat) + H^{+} + 2e^{-} \qquad (7)$$

This suggestion fits the experimental data in two respects. First it predicts a slope of 0.029 volts per pH unit in the graph of $E_{1/2}$ *vs.* pH. The observed slope in Fig. 3 is 0.032 volts per pH unit. Second, it would account for the fact that the wave is not observed at low pH values where complex formation is expected to be very weak or non-existent.

CHAPTER II

THE POLAROGRAPHY OF IRON-CATECHOL COMPLEXES

INTRODUCTION

It has been recognized for some time that aromatic vic-diols such as catechol can form very stable complexes with ferric ions[18], and they are known to play a role in assimilation, storage, and transport of iron in certain microorganisms. As availability of iron is extremely limited in the environment due to the insolubility of ferric hydroxide, low molecular weight chelating compounds called siderophores are often manufactured by microorganisms to facilitate the uptake and transport of ferric ion.[19-21] For example, enterobactin, the principle siderophore of enteric bacteria, is a molecule that contains three aromatic vic-diol groups oriented in such a way that all three can coordinate to a single ferric ion. It is estimated[23] to have a formation constant with ferric ion on the order of 10^{45}.

On the other hand, Mentasti et al[22] showed that Fe^{3+} oxidizes catechol in acidic solutions forming Fe^{2+} and ortho-quinone:

$$2\ Fe^{3+} + H_2cat \rightleftharpoons 2\ Fe^{2+} + qn + 2\ H^+ \qquad (8)$$

An esr study[23] indicated some oxidation of the catechol by Fe^{3+} at pH as high as 4. At still higher pH, because catechol complexes Fe^{3+} much more strongly than Fe^{2+}, the trivalent state is stabilized and the equilibrium in Eq. 8 shifts far to the left.

A potentiometric titration study[23] of Fe(III)-catechol

complexes gave the following formation constants:

$$K_1 = 10^{20.01} = \frac{[Fe(cat)^+]}{[Fe^{3+}][cat^{2-}]} \quad (9)$$

$$K_2 = 10^{14.69} = \frac{[Fe(cat)_2^-]}{[Fe(cat)^+][cat^{2-}]} \quad (10)$$

$$K_3 = 10^{9.06} = \frac{[Fe(cat)_3^{3-}]}{[Fe(cat)_2^-][cat^{2-}]} \quad (11)$$

at t=27.1°C and μ=0.08, where [ ] represents molar concentration.

Equilibrium constants for Fe(II)-catechol complexes were reported by Martell and Tyson[24] as follows:

$$K_1^* = 10^{-14.332} = \frac{[Fe(cat)][H^+]^2}{[Fe^{2+}][H_2cat]} \quad (12)$$

$$K_2^* = 10^{-16.740} = \frac{[Fe(cat)_2^{2-}][H^+]^2}{[Fe(cat)][H_2cat]} \quad (13)$$

at t=25°C and μ=1.0 (KNO_3).

Knowing the proton dissociation constants of catechol,[23]

$$K_{a1} = 10^{-9.22} = \frac{[Hcat^-][H^+]}{[H_2cat]} \quad (14)$$

$$K_{a2} = 10^{-13.00} = \frac{[H^+][cat^{2-}]}{[Hcat^-]} \quad (15)$$

one can derive the distribution curves of catechol, Fe(II)-catechol complexes, and Fe(III)-catechol complexes. These results are given in Figs. 6, 7 and 8.

Although data on the formation constants of both Fe(II) and Fe(III)-catechol complexes are available from the potentiometric titration method, none is found from polarographic work. Especially, the information on Fe(II)-catechol chemistry is extremely limited. Therefore, the calculation of the formation constants

of Fe(II)-catechol complexes from a polarographic study was chosen as the final goal of the present work.

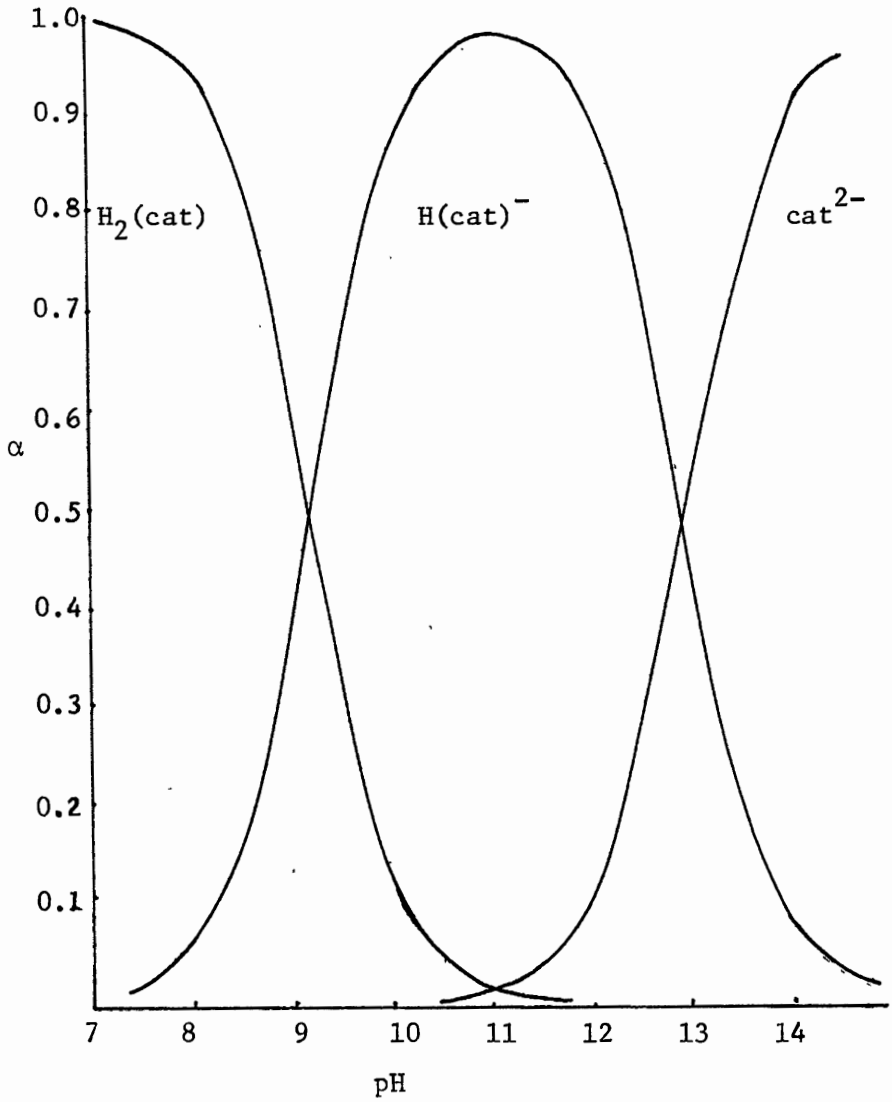

Figure 6. Distribution of catechol species as a function of pH.

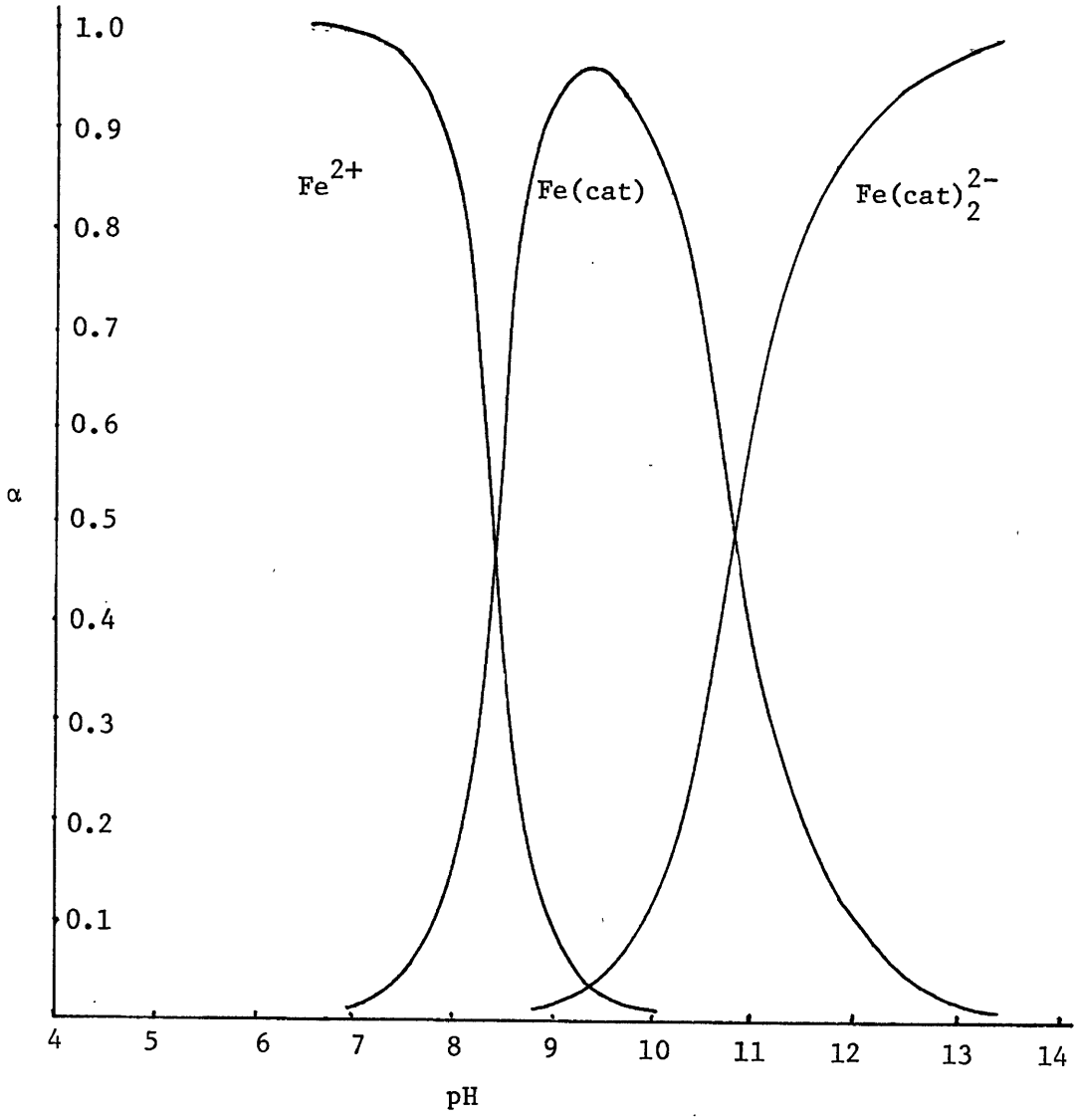

Figure 7. Distribution of Fe(II)-catechol complexes as a function of pH. The concentrations are: 5.01×10^{-3}F of catechol and 1.03×10^{-3}F of Fe(II).

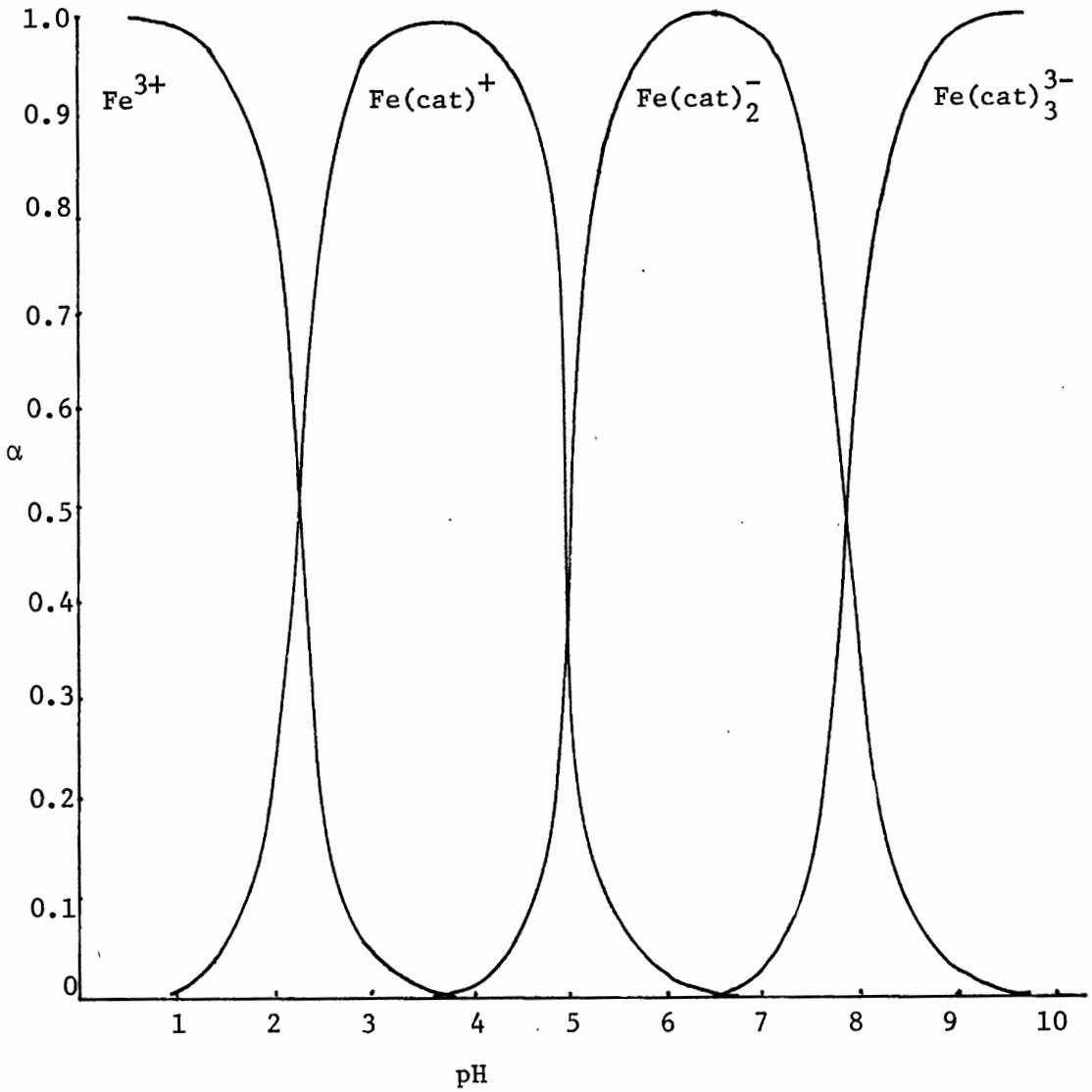

Figure 8. Distribution of Fe(III)-catechol complexes as a function of pH. The concentrations are 5.00×10^{-3}F of catechol and 1.05×10^{-3}F of Fe(III).

EXPERIMENTAL

Materials

Hexahydrated ferrous perchlorate, $Fe(ClO_4)_2 \cdot 6H_2O$, and anhydrous ferric perchlorate, $Fe(ClO_4)_3$, were both reagent grade and obtained from G. Frederick Smith. The ferric perchlorate was used only after ferric hydroxide was removed by filtration through a membrane filter having 0.45 micron pore size.

Other materials such as catechol, Triton X-100, and sodium perchlorate were the same as described in Chapter I.

Polarography of Fe(III) in the Presence of Catechol

A solution of 2×10^{-3} F iron(III) perchlorate in 0.100 F sodium perchlorate was prepared. The pH of the sodium perchlorate solution was adjusted to 2 with 60% perchloric acid before adding iron(III) perchlorate in order to avoid forming a precipitate of $Fe(OH)_3$. A second solution, 1×10^{-2} F in catechol, was prepared in 0.100 F sodium perchlorate. To measure a polarogram, 25.00 ml of the above catechol solution was taken, the pH adjusted to about 7 with 10 M NaOH, and then 25.00 ml of the ferric perchlorate solution added. While adding the ferric perchlorate solution, it was necessary to monitor the pH closely because oxidation of catechol will occur if the pH drops below 4 or 5. Next, 2.0 ml of 0.4% Triton X-100 was added and the pH adjusted to the desired value by adding 10 M NaOH with a 10 microliter syringe. A fresh

solution was prepared for each different pH studied.

Polarography of Fe(II) in the Presence of Catechol

A Fe(II) stock solution, 1×10^{-3} F, was prepared by dissolving ferrous perchlorate hexahydrate in 0.100 F $NaClO_4$ which had been deoxygenated by flushing with nitrogen and acidified with 60% perchloric acid to a pH of 2. A Fe(II)-catechol solution was then prepared under a nitrogen atmosphere by adding about 270 mg of solid catechol to a 1000-ml round bottom flask, followed by 500 ml of the ferrous perchlorate stock solution. This produces a Fe(II)-catechol solution that is 5.01×10^{-3} F in catechol and 1.03×10^{-3} F in Fe(II).

To measure a polarogram, a 25.00 ml aliquot of Fe(II)-catechol stock solution was transferred to the cell followed by 1.5 ml 0.2% Triton X-100. The pH was adjusted by adding 10 M sodium hydroxide with a 10 microliter syringe. After bubbling nitrogen through the solution for 10 minutes the polarogram was recorded.

RESULTS AND DISCUSSION

Reduction of Fe(III) in the Presence of Catechol

Two waves are expected for the reduction of Fe(III):

$$Fe(cat)_p^{3-2p} + e^- = Fe(cat)_q^{2-2q} + (p-q)\ cat^{2-} \quad (16)$$

$$Fe(cat)_q^{2-2q} + 2\ e^- = Fe(s) + q\ cat^{2-} \quad (17)$$

The first wave corresponds to the one electron reduction of trivalent iron to divalent iron. The second wave is due to a two electron reduction of divalent iron to iron metal. According to the Ilkovic equation, the limiting current is proportional to the number of electrons exchanged, so the limiting current of the second wave is expected to be twice that of the first wave.

Reduction waves of Fe(III) in the presence of catechol are shown in Fig. 9. At pH 11.6 and 12.0, two steps are recorded, and the height of the second wave is about twice that of the first wave, as expected. It is therefore postulated that the first wave is due to Fe(III)→Fe(II) (Eq. 16) and the second wave is due to Fe(II)→Fe(s) (Eq. 17). The shift of the first wave is from about +0.55 volts (vs. SCE) for uncomplexed Fe^{3+} to about -1.6 volts (vs. SCE) for Fe(III) complexed with catechol at pH about 12, an unusually large shift of the half-wave potential. The reduction of uncomplexed Fe^{2+} occurs at about -1.4 volts (vs. SCE) and is shifted to about -1.8 volts (vs. SCE) by complex formation with catechol at pH about 12. At pH below 11.6 the two waves are

apparently too close together to be resolved.

Oxidation and Reduction of Fe(II) in the Presence of Catechol

Two waves with 1:2 step height ratio are expected: a one electron oxidation wave (the reverse of Eq. 16), and a two electron reduction wave according to Eq. 17.

Oxidation of Fe(II) in the Presence of Catechol

The oxidation waves at various pH values can be seen in Fig. 10 and this portion of the polarogram is expanded in Fig. 11. Data for these waves are summarized in Table III.

TABLE III

THE OXIDATION OF IRON(II)-CATECHOL COMPLEXES AT THE DROPPING MERCURY ELECTRODE. CONCENTRATIONS ARE: 1.03×10^{-3} F OF IRON(II), 5.01×10^{-3}F OF CATECHOL

pH	i_d obs. at E_d* (microamp.)	E_d vs. SCE (volts)	$E_{1/2}$** vs. SCE (volts)	$\frac{0.059}{n\alpha}$ (volts)	α
5.22	0.3	0.14	0.06	-	-
7.24	0.2	0.00	-0.28	-	-
8.45	1.53	-0.10	-0.454	0.159	0.37
9.76	2.81	-0.15	-0.568	0.193	0.31
10.64	2.46	-0.20	-0.591	0.177	0.33
11.92	2.28	-0.30	-0.627	0.175	0.34
12.00	2.15	-0.36	-0.658	0.178	0.33
12.30	1.98	-0.40	-0.690	0.175	0.34

*E_d = the potential at which i_d was measured.
** See Eq. 6

In the absence of complex formation the reversible oxidation of Fe^{2+} will occur at a potential of about +0.55 volts (vs. SCE), which is outside the range accessible with a dropping mercury electrode. In the presence of complexing agent this voltage may

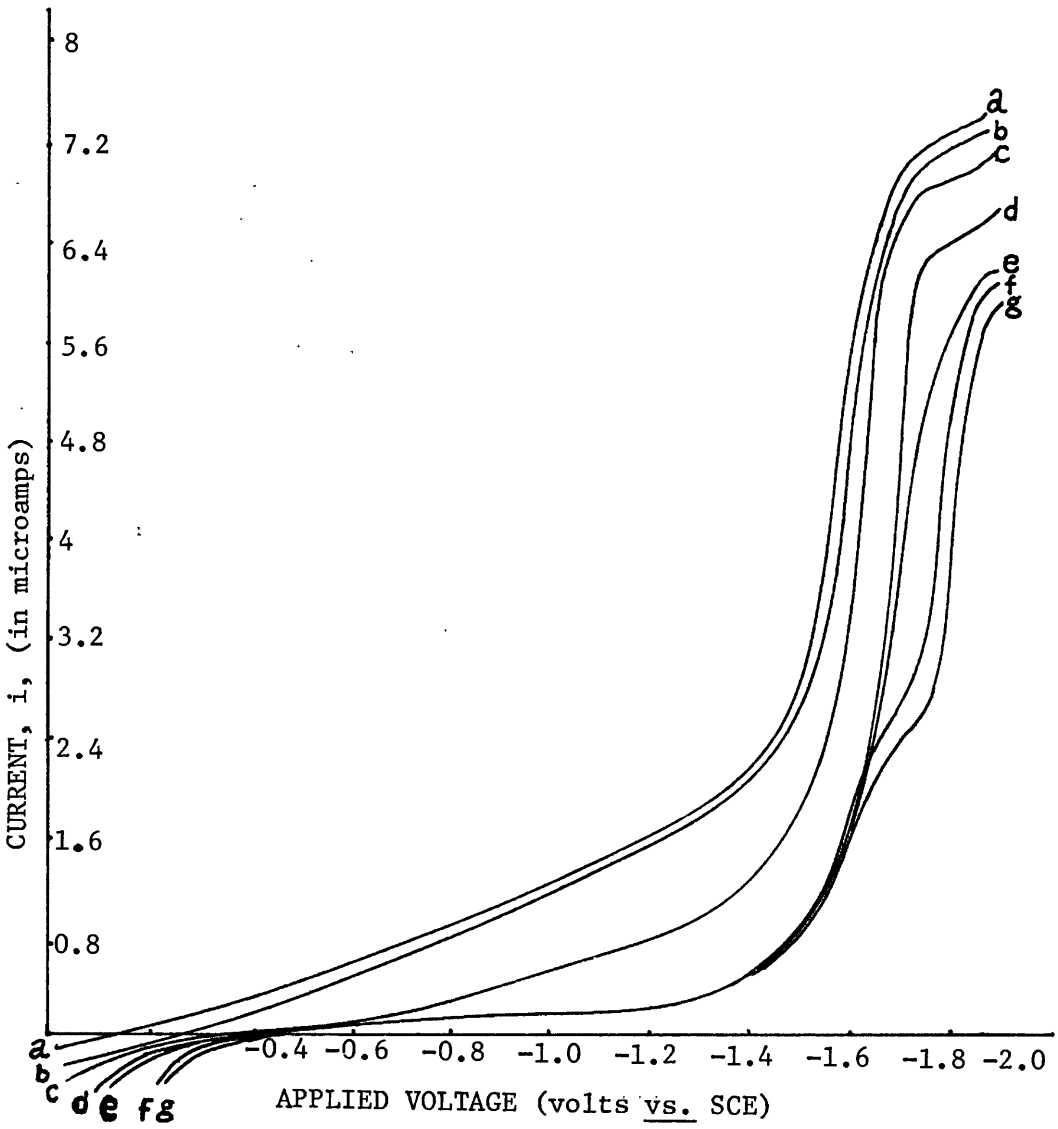

Figure 9. Cathodic waves of Fe(III) in the presence of catechol at following pH a) 5.25 b) 7.42 c) 8.47 d) 10.04 e) 11.04 f) 11.60 g) 11.95 (the concentrations are: 1.05×10^{-3}F of Fe(III) and 5.00×10^{-3}F of catechol).

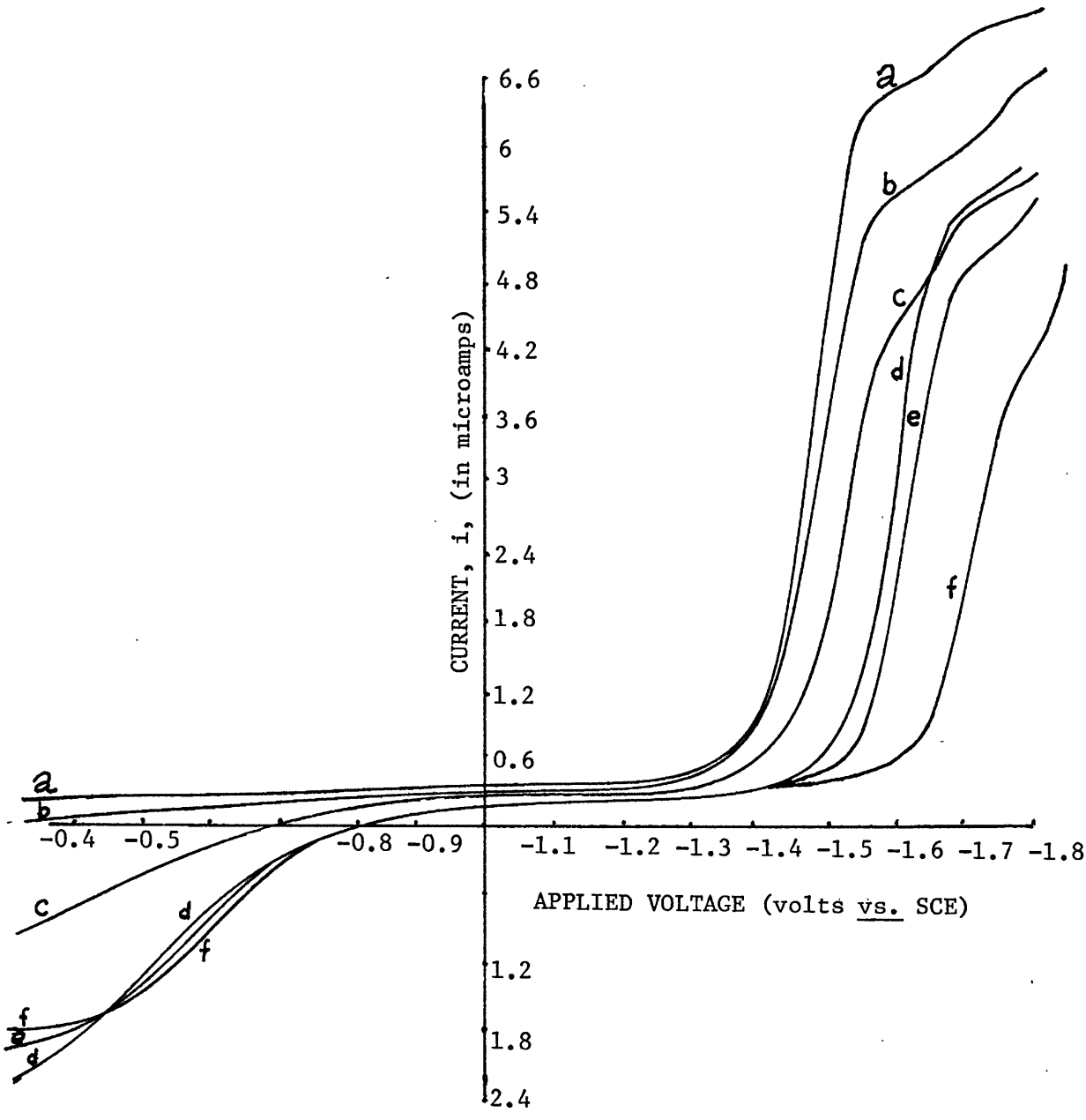

Figure 10. Current-voltage curves of Fe(II) in the presence of catechol at following pH a) 3.95 b) 5.22 c) 8.45 d) 9.76 e) 10.64 f) 11.92 (the concentrations are: 1.03×10^{-3}F of Fe(II) and 5.02×10^{-3}F of catechol).

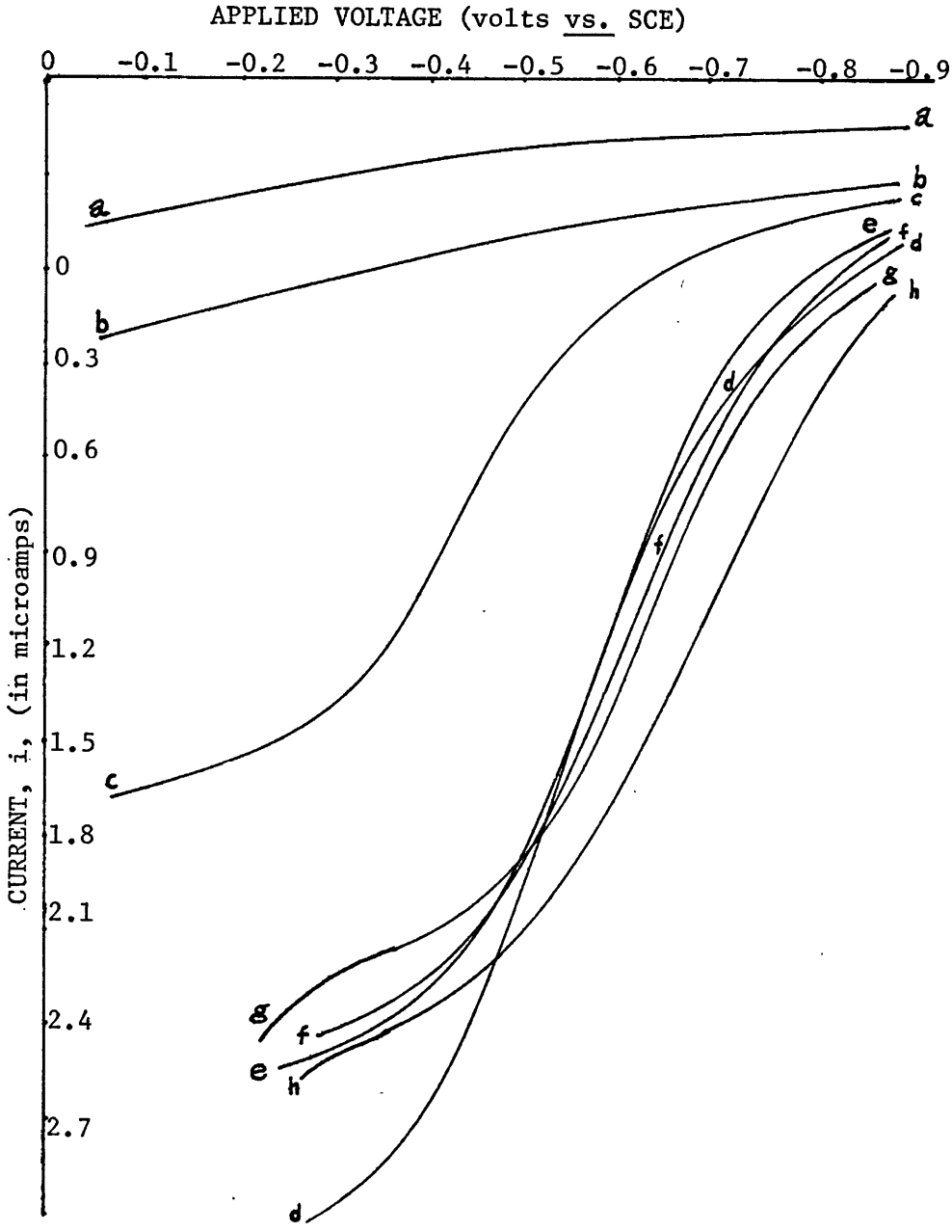

Figure 11. Oxidation waves of Fe(II) in the presence of catechol at following pH a) 3.95 b) 5.22 c) 8.45 d) 9.76 e) 10.64 f) 11.92 g) 12.00 h) 12.30 (the concentrations are: 1.03×10^{-3}F of Fe(II) and 5.01×10^{-3}F of catechol).

be shifted to more positive values if iron(II) is complexed more strongly than iron(III), or (as observed in the present case) to more negative values if iron(III) is complexed more strongly than iron(II).

In the presence of catechol, because iron(III) is complexed more strongly than iron(II), the oxidation waves of iron(II) are shifted to more negative potentials upon complexation. The variations of i_d and $E_{\frac{1}{2}}$ as a function of pH are plotted in Fig. 12 and Fig. 13. The curve in Fig. 12 looks very similar to the distribution curve of Fe(cat) (see Fig. 7). The diffusion coefficient, D, calculated from i_d at pH 9.76 is 5.3×10^{-6} $cm^2 sec^{-1}$, which seems to be a normal value for a complex such as Fe(cat). It is suggested that only Fe(cat) is oxidized and observed here.

In Fig. 13, the general shape of the pH dependence curve can be understood from the following electrode reactions involving the predominant species in solution:

$$Fe(cat) = Fe(cat)^{+} + e^{-} \quad (pH<5) \qquad (18)$$

$$Fe(cat) + H_2cat = Fe(cat)_2^{-} + 2H^{+} + e^{-} \quad (5<pH<8) \qquad (19)$$

$$Fe(cat) + 2Hcat^{-} = Fe(cat)_3^{3-} + 2H^{+} + e^{-} \quad (9<pH<13) \qquad (20)$$

$$Fe(cat) + 2cat^{2-} = Fe(cat)_3^{3-} + e^{-} \quad (13<pH) \qquad (21)$$

at pH below 5 and above 13, no hydrogen ion is produced as shown in Eqs. 18 and 21, and the half-wave potential approaches pH independence. Between pH 5 and 13, the half-wave potential is shifted to more negative values as pH increases. Therefore the curve in Fig. 13 is qualitatively explained.

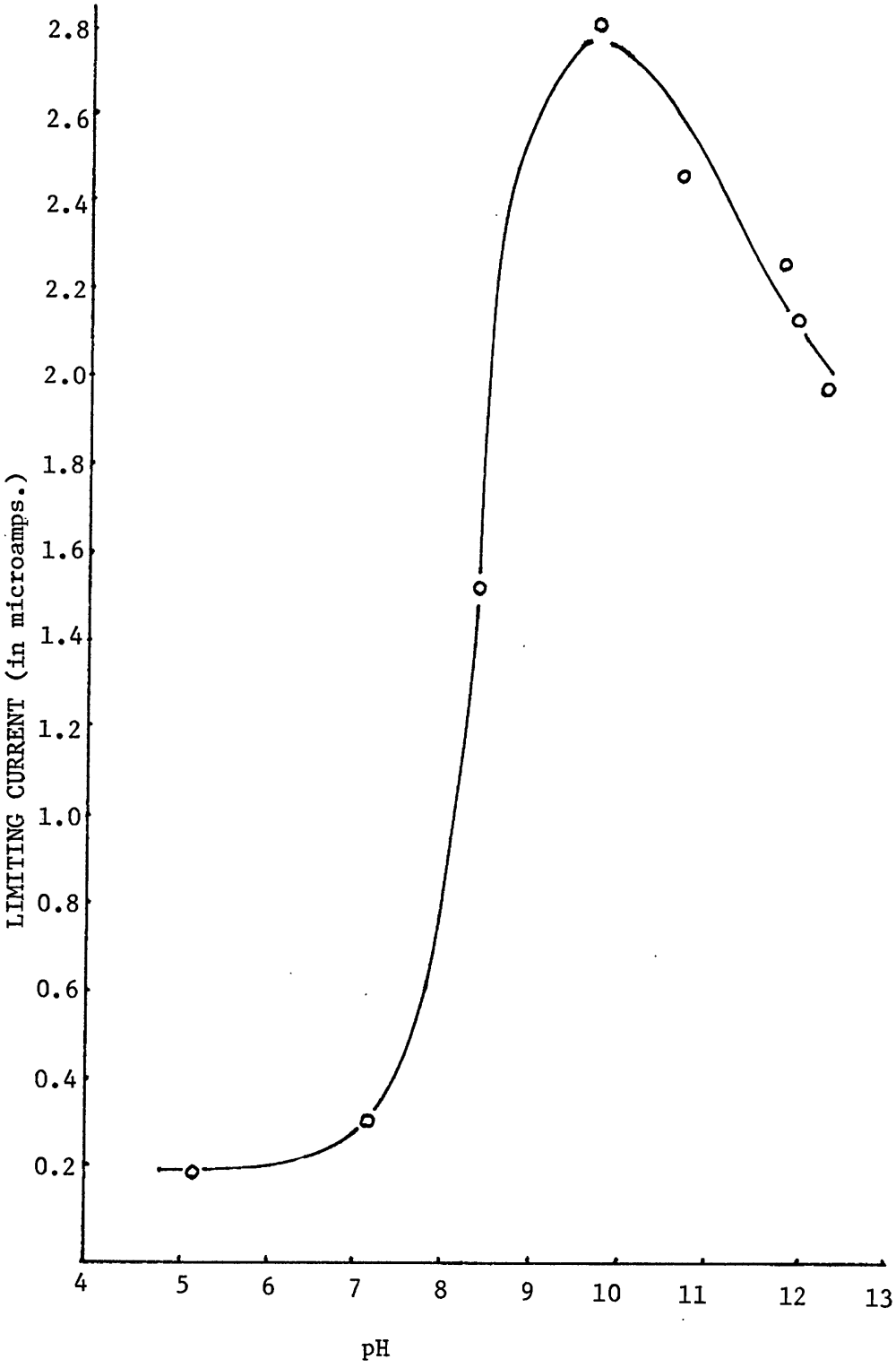

Figure 12. Effect of pH on limiting current of anodic wave of Fe(II)-catechol complex. The concentrations of this test solutions are: 1.03×10^{-3}F in Fe(II) and 5.01×10^{-3}F in catechol.

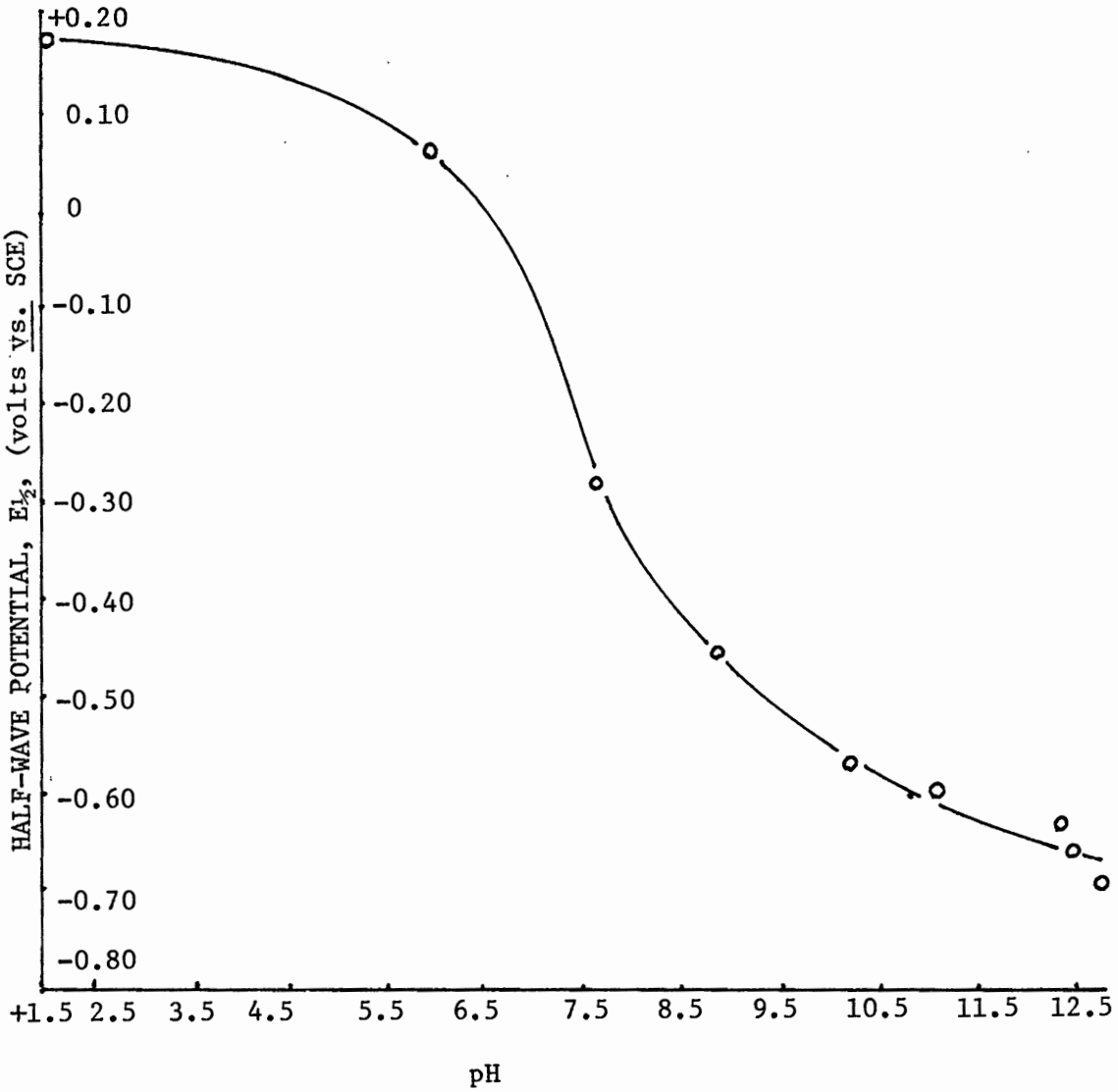

Figure 13. Influence of pH on the half-wave potential of Fe(II) catechol oxidation wave. Text solution is 1.03 x 10^{-3}F in Fe(II) and 5.01 x 10^{-3}F in catechol.

Reduction of Fe(II) in the Presence of Catechol

The reduction of Fe(II) in the presence of catechol is expressed in Eq. 17. The waves due to the reduction of Fe(II)-catechol complexes to metallic iron in Fig. 10 are expanded in Fig. 14. Data for these waves are reported in Table IV.

TABLE IV

REDUCTION OF IRON(II)-CATECHOL AT THE DROPPING MERCURY ELECTRODE

pH	i_d obs. at E_d (microamp.)	E_d vs. SCE (in volts)	$E_{1/2}$ vs. SCE (in volts)	$\frac{0.059}{n\alpha}$ (in volts)	α
3.95	7.87	-1.66	-1.493	0.067	0.44
7.24	6.58	-1.66	-1.488	0.073	0.40
8.45	5.47	-1.68	-1.537	0.085	0.35
9.76	6.53	-1.80	-1.601	0.069	0.43
10.64	6.17	-1.78	-1.628	0.052	0.57
11.92	4.94	-1.84	-1.746	0.074	0.40
12.00	3.66	-1.92	-1.784	0.058	0.51
12.30	3.60	-1.92	-1.814	0.056	0.53

From the results in Table IV it appears that the electrolytic reduction of Fe(II)-catechol complexes to metallic iron is irreversible with α ranging from 0.35 to 0.57. It is also shown that the half-wave potential is progressively shifted to more negative values as pH increases. In spite of the fact that this wave is irreversible, there is at least a possibility of using the shift of $E_{1/2}$ to measure the formation constants.[25-27]

Calculation of Formation Constants of Fe(II)-Catechol Complexes

It is attempted here to use the Fe(II)→Fe(s) wave for the calculation of the formation constants β_1 and β_2 of Fe(II)-

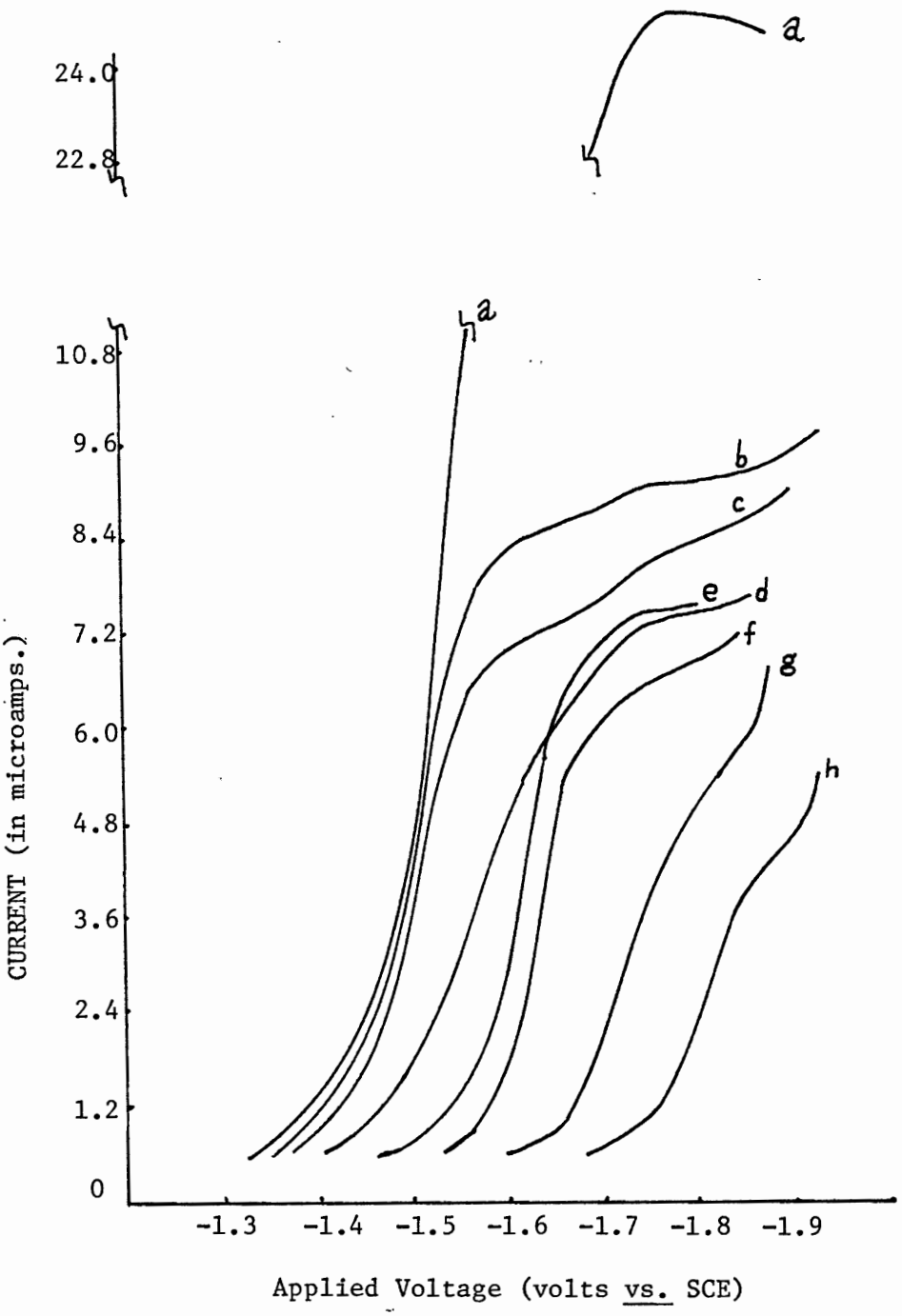

Figure 14. Reduction waves of Fe(II) in the presence of catechol at following pH: a) 2.90 b) 3.95 c) 7.24 d) 8.45 e) 9.76 f) 10.64 g) 11.92 h) 12.30. (The concentrations are: 1.03×10^{-3}F of Fe(II) and 5.01×10^{-3}F of catechol.)

catechol complexes

$$\beta_1 = \frac{(Fe(cat))}{(Fe^{2+})(cat^{2-})} \tag{22}$$

$$\beta_2 = \frac{(Fe(cat)_2^{2-})}{(Fe^{2+})(cat^{2-})^2} \tag{23}$$

where ( ) represents the activity. Because (cat^{2-}) depends on pH it is necessary to take the proton association constants of catechol, β_1^H and β_2^H, into account.

$$\beta_1^H = \frac{(Hcat^-)}{(cat^{2-})(H^+)} \tag{24}$$

$$\beta_2^H = \frac{(H_2cat)}{(cat^{2-})(H^+)^2} \tag{25}$$

The following equation which relates the shift in half-wave potential, $\Delta E_{\frac{1}{2}}$, to the complex formation constant, β_j, is applied to the present work:

$$\exp\left\{\frac{-\Delta E_{\frac{1}{2}} \alpha n F}{RT}\right\} = \gamma_{Fe^{2+}}\left\{\frac{1}{\gamma_{Fe^{2+}}} + \frac{\beta_1}{\gamma_{Fe(cat)}}\left(\frac{T_{cat}}{*_\Sigma}\right) + \frac{\beta_2}{\gamma_{Fe(cat)_2^{2-}}}\left(\frac{T_{cat}}{*_\Sigma}\right)^2 + \cdots\right\} \tag{26}$$

where $\Delta E_{\frac{1}{2}}$ = the shift of half-wave potential upon complex formation

α = electron transfer coefficient

γ = activity coefficient

T_{cat} = total concentration of catechol

$*_\Sigma = \sum_{p=0}^{2} \frac{\beta_p^H (H^+)^p}{\gamma_{H_p cat}^{p-2}}$, p=0, 1 or 2 in case of cat^{2-}, $Hcat^-$ or H_2cat respectively.

The derivation and the application of Eq. 26 are given in the appendix.

A graph of $E_{1/2}$ against pH is shown in Fig. 15. The curve can be divided into three segments depending on whether Fe^{2+}, Fe(cat) or $Fe(cat)_2^{2-}$ is the predominant species in solution.

The first segment with pH values lower than 7.7 is horizontal. Free ferrous ion is assumed to be the predominant specie in this region. No complexation occurs and therefore no shift in $E_{1/2}$ is expected. In the second segment ranging from pH 7.7 to 11.8, $E_{1/2}$ is shifted to more negative potential, and it is assumed to be due to the occurrence of 1:1 complex formation in this pH range. From pH 11.8 to at least 12.3 the profound affect of pH on $E_{1/2}$ is assumed to be due to the formation of the 1:2 Fe(II)-catechol complex. With these assumptions it is possible to calculate the formation constants β_1 and β_2 using Eq. 26.

The shift in $E_{1/2}$ is first calculated according

$$\Delta E_{1/2} = E_{1/2}' - E_{1/2} \tag{27}$$

where $E_{1/2}$ and $E_{1/2}'$ are the half-wave potential of the reduction wave of uncomplexed Fe^{2+} and complexed Fe(II) respectively. A value of -1.490 (vs. SCE) volts for $E_{1/2}$ of uncomplexed Fe^{2+} was taken from the $E_{1/2}$ value at low pH where there is no complex formation. With these data, one can calculate $\Delta E_{1/2}$ and also $\exp\left\{\frac{-\Delta E_{1/2}\alpha nF}{RT}\right\}$. These values at 25°C are reported in Table V.

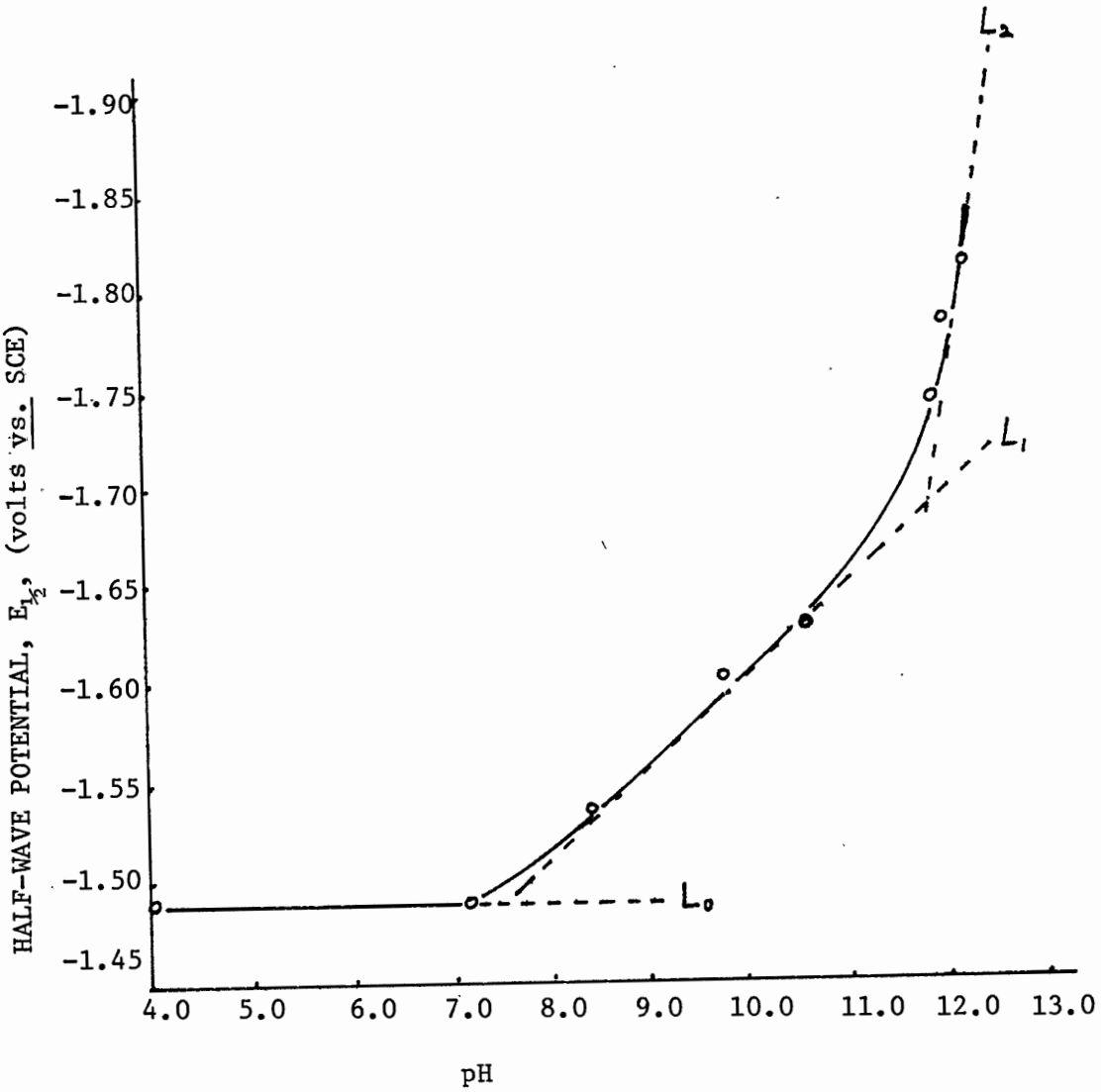

Figure 15. Variation of the half-wave potential of Fe(II) cathodic wave as a function of pH in the presence of catechol. The concentrations are: 1.03×10^{-3}F of Fe(II) and 5.01×10^{-3}F catechol.

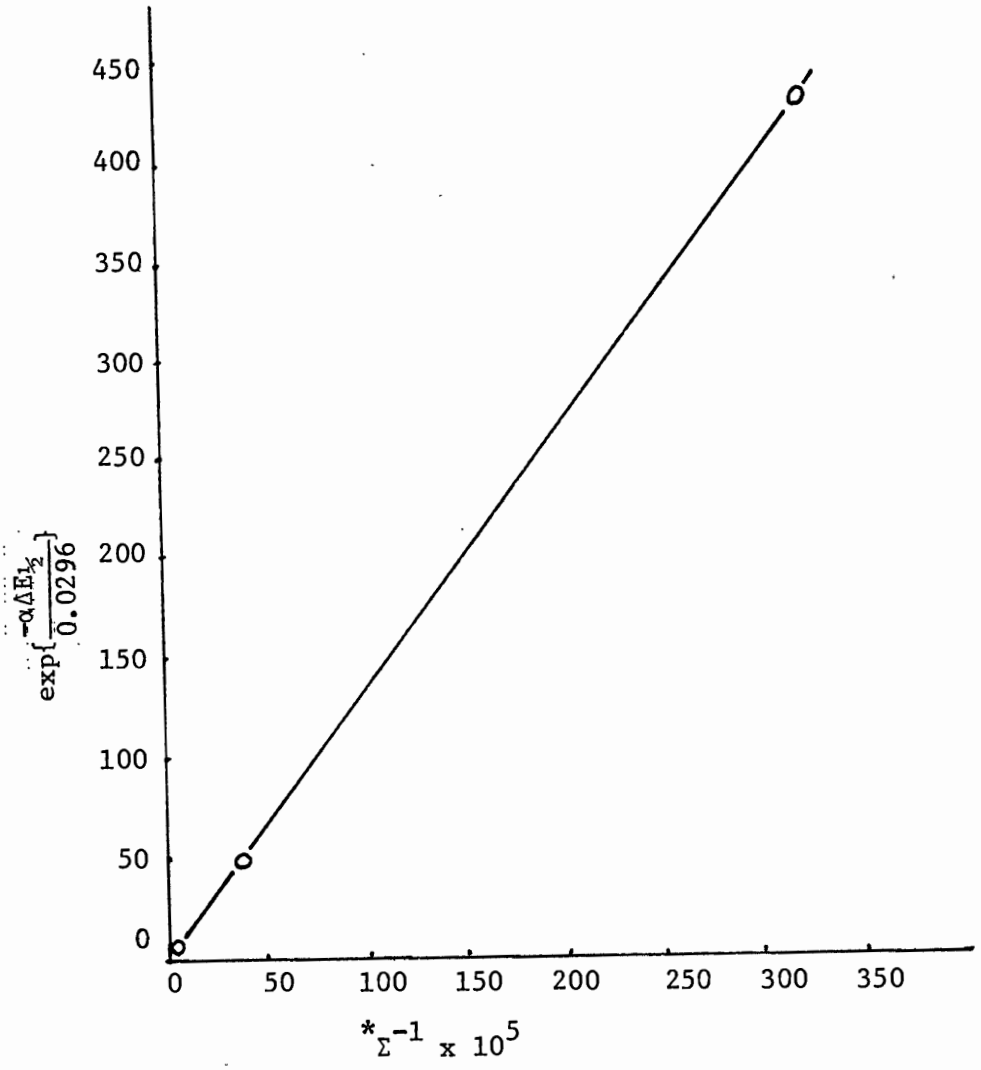

Figure 16. The calculation of stability constant of Fe(cat), β_1.

TABLE V

CALCULATION OF STABILITY CONSTANT β_1

pH	α	$\Delta E_{\frac{1}{2}}$ (in volts)	$\exp\left\{\frac{-\alpha\,\Delta E_{\frac{1}{2}}}{0.0296}\right\}$	$*_\Sigma^{-1}$
8.45	0.345	-0.047	3.53	3.96×10^{-6}
9.76	0.440	-0.113	47.8	3.61×10^{-4}
10.64	0.565	-0.138	431	3.23×10^{-3}
11.92	0.400	-0.256	2.88×10^{3}	5.44×10^{-2}
12.00	0.510	-0.294	1.16×10^{5}	6.41×10^{-2}
12.30	0.525	-0.324	5.58×10^{5}	1.09×10^{-1}

$\beta_1^H = 10^{-13.00}$ and $\beta_2^H = 10^{-22.22}$ were used in the calculation of $*_\Sigma^{-1}$.

Assuming that the 1:1 complex is predominant over the pH range from 7.7 to 11.8, Eq. 26 is reduced to

$$\exp\left\{\frac{-\Delta E_{\frac{1}{2}}\alpha nF}{RT}\right\} = \gamma_{Fe^{2+}}\left\{\frac{1}{\gamma_{Fe^{2+}}} + \frac{\beta_1}{\gamma_{Fe(cat)}}\left(\frac{Tcat}{*_\Sigma}\right)\right\} \qquad (28)$$

Therefore, a graph of $\exp\left\{\frac{-\Delta E_{\frac{1}{2}}\alpha nF}{RT}\right\}$ <u>vs.</u> $*_\Sigma^{-1}$ will be a straight line with slope defined as

$$\text{slope} = \beta_1\, T_{cat}\, \gamma_{Fe^{2+}}/\gamma_{Fe(cat)} \qquad (29)$$

Such a plot is given in <u>Fig. 16</u> and the slope is found to be equal to 1.3×10^5. Calculation of the activity coefficients was accomplished by Eq. 30:

$$-\log \gamma_1 = \tfrac{1}{2} Z_i^2\{\sqrt{\mu}/(1+\sqrt{\mu}) - 0.2\mu\} \qquad (30)$$

Under the present experimental condition, $\mu = 0.100$, the values of $\gamma_{Fecat_2^{2j-2}}$ are calculated to be:

$$\gamma_{Fe^{2+}} = \gamma_{Fecat_2^{2-}} = \gamma_{cat^{2-}} = 0.363$$
$$\gamma_{Fecat} = \gamma_{H_2cat} = 1.00$$
$$\gamma_{Fecat_3^{4-}} = 0.017 \qquad (31)$$
$$\gamma_{Hcat^-} = 0.776$$

Substituting the appropriate values for $\gamma_{Fe^{2+}}$, γ_{Fecat} into Eq. 29 a value of 7×10^7 is obtained for β_1.

Over the pH range from 11.9 to 12.3, the 1:2 complex is predominant in solution. Under this condition Eq. 26 can be written as:

$$*_\Sigma\left\{\exp\left(\frac{-\Delta E_{\frac{1}{2}}\alpha nF}{RT}\right) - 1\right\} = \frac{\beta_1\gamma_{Fe^{2+}}}{\gamma_{Fe(cat)}} T_{cat} + \frac{\beta_2\gamma_{Fe^{2+}}}{\gamma_{Fe(cat)_2^{2-}}}\left(\frac{T_{cat}^2}{*_\Sigma}\right) \qquad (32)$$

A graph of $*_\Sigma\left\{\exp\left(\frac{-\Delta E_{\frac{1}{2}}\alpha nF}{RT}\right)-1\right\}$ vs. $*_\Sigma^{-1}$ will be a straight line with slope given by:

$$\text{slope} = \beta_2 T_{cat}^2 \gamma_{Fe^{2+}}/\gamma_{Fe(cat)_2^{2-}} \qquad (33)$$

Such a plot is shown in Fig. 17 and data are summarized in Table VI.

TABLE VI

CALCULATION OF FORMATION CONSTANT β_2

pH	α	$\Delta E_{\frac{1}{2}}$	$\exp\left\{\frac{-\Delta\alpha E_{\frac{1}{2}}}{0.0296}\right\}$	$*_\Sigma^{-1}$	$*_\Sigma\left\{\exp\left(\frac{-\alpha\Delta E_{\frac{1}{2}}}{0.0296}\right)-1\right\}$
11.92	0.400	-0.256	0.288×10^4	5.47×10^{-2}	5.16×10^4
12.00	0.510	-0.294	11.6×10^4	6.41×10^{-2}	1.81×10^6
12.30	0.525	-0.324	55.8×10^4	1.09×10^{-1}	5.14×10^6

A slope of 8.8×10^7 is found from Fig. 17 and β_2 is calculated to be 4×10^{12} according to Eq. 33.

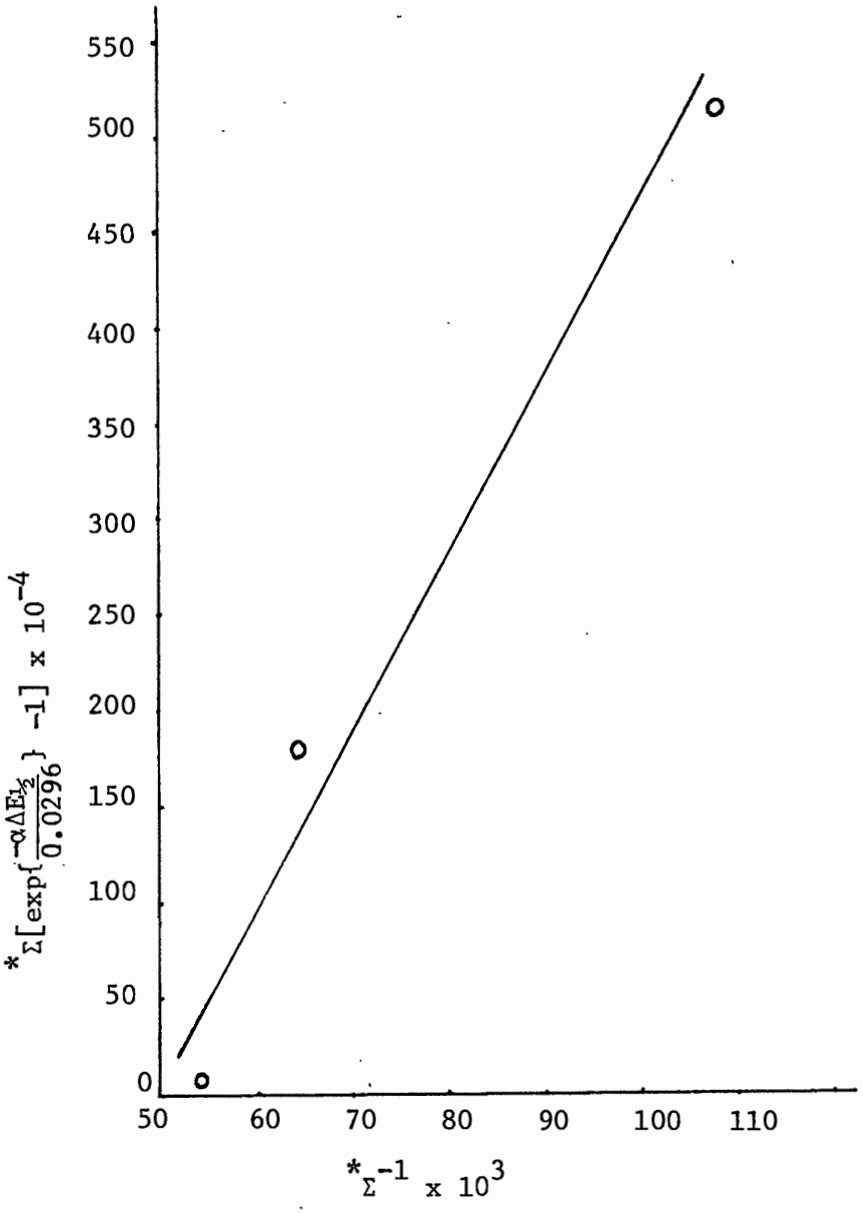

Figure 17. The calculation of the stability constant of $Fe(cat)_2^{2-}$, β_2.

By using pK_{a1} = 9.22 and pK_{a2} = 13.00 for catechol, the complex formation constants K_1^* and K_2^* reported by Martell and Tyson[24] can be converted into β_1 and β_2. The results are

$$\beta_1 = 8 \times 10^7 \text{ and } \beta_2 = 3 \times 10^{13} \text{ compared with}$$

$$\beta_1 = 7 \times 10^7 \text{ and } \beta_2 = 4 \times 10^{12} \text{ from the present work.}$$

Eq. 26 which was applied to the present work for the calculation of β_1 and β_2 is valid under the condition, $T_{cat} >> T_{Fe}$, as pointed out in the Appendix. However, because $T_{cat} = 5.03 \times 10^{-3}$ F and $T_{Fe} = 1.03 \times 10^{-3}$ F, this condition was not strickly fulfilled. As a result, only crude values of β_1 and β_2 are reported here.

REFERENCES

1. A.E. Martell, Pure Appl. Chem., 17, 129 (1968).
2. J. Halpern, Discuss. Faraday Soc., No 46, 7 (1968).
3. J. Halpern, Pure Appl. Chem., 20, 59 (1969).
4. J. Kochi, Science, 155, 415 (1967).
5. B.R. Brown, in "Oxidative Coupling of Phenols," W.I. Taylor and A.R. Battersby, Eds., Marcel Dekker, Inc., New York, New York, (1967), p. 197.
6. G.A. Hamilton, Adv. Enzymol., 59, 55 (1969).
7. G.M. Fair, J.C. Geyer, and D.A. Okun, "Waste and Wastewater Engineering," Vol. II, Wiley, New York, N.Y. (1968).
8. R.W. Holcomb, Science, 169, 457 (1970).
9. M.A. Joslyn and G.E.K. Branch, J. Am. Chem. Soc., 57, 1779 (1935).
10. J.R. Gillette, D. Eatland, and G. Kalnitsky, Biochim. Biophys. Acta, 15, 526 (1954).
11. R.R. Grinstead, Biochemistry, 3, 1308 (1964).
12. C.A. Tyson and A.E. Martell, J. Am. Chem. Soc., 94, 939 (1972).
13. L. Sommer and L. Benisek, Coll. Czech. Chem. Comm., 22, 166 (1957).
14. J. Doskocil, Coll. Czech. Chem. Comm., 15, 599 (1950).
15. A.K. Vlcek, V. Mansfeld, and D. Kryskova, Collegium, No. 874, 245 (1943).
16. C.M. Wheeler and R.P. Vigneault, J. Am. Chem. Soc., 74, 5232 (1952).
17. J. Doskocil, Coll. Czech. Chem. Comm., 15, 780 (1950).
18. G. Vogler, Arch. Exp. Pathol. Pharmakol., 194, 281 (1940).
19. J.B. Neilands, Ed., "Microbial Iron Metabolism," Academic Press, New York, New York (1974).

20. J.B. Neilands, "Inorganic Biochemistry," G. Eichorn, Ed., Elsevier, New York, New York (1973), p. 167.

21. C.E. Lankford, "CRC Critical Reviews in Microbiology," 2, 273 (1973).

22. E. Mentasti and E. Pelizzetti, J. Chem. Soc., Dalton, 23, 2605 (1973).

23. A Avdeef, S.R. Sofen, T.L. Bregante, K.N. Raymond, J. Am. Chem. Soc., 100, 5362 (1978).

24. C.A. Tyson and A.E. Martell, J. Am. Chem. Soc., 90, 3379 (1968).

25. R. Brdicka, Coll. Czech. Chem. Comm., Suppl. II, 19, 41 (1954).

26. J. Biernat and M. Baranowska-Zralko, Electrochimica Acta, 17, 1867 (1972).

27. M. Baranowska-Zratko and J. Biernat, Electrochimica Acta, 17, 1877 (1972).

28. C.R. Dawson and J.M. Nelson, J. Am. Chem. Soc., 60, 250 (1938).

29. J.O. Howden and G.F. Reynolds, J. Polarographic Soc., 11, 3 (1965).

30. H. Irving "Advances in Polarography," 1, 50 (1959).

31. V.F. Ivanov and Z.A. Iota Russian J. Phy. Chem., 37(a), 1156 (1963).

32. P. Zuman "The Eluciation of Organic Electrode Process," p. 11, Academic Press, New York, London (1969).

33. E.G. Ball and T.T. Chen, J. Biol. Chem., 102, 691 (1932).

APPENDIX

EVALUATION OF STABILITY CONSTANTS FROM AN IRREVERSIBLE POLAROGRAPHIC WAVE

The reduction of the simple ion to a metal that is insoluble in mercury, e.g., Fe^{2+}, may be represented by

$$Fe^{2+} + 2\ e^{-} = Fe(s) \qquad \text{(A-1)}$$

Assuming that the activity of the deposited metal on the surface of the dropping electrode is constant, then $E_{d.e.}$ at any point on the wave should depend only on the activity of the metal ion in the solution, and should be given by

$$E_{d.e.} = E^{o}_{Fe^{2+}\rightarrow Fe(s)} + \frac{RT}{\alpha nF} \ln(Fe^{2+})^{o} \qquad \text{(A-2)}$$

where $E^{o}_{Fe^{2+}\rightarrow Fe(s)}$ is the ordinary standard half-cell potential of the $Fe^{2+}\rightarrow Fe(s)$ couple, and $(Fe^{2+})^{o}$ is the activity of Fe^{2+} at the surface of the dropping electrode. Because the reduction of Fe^{2+} is known to be irreversible[31] the electron transfer coefficient, α, is introduced. The current at any point on the wave is given by

$$i = k\{[Fe^{2+}] - [Fe^{2+}]^{o}\} \qquad \text{(A-3)}$$

where $[Fe^{2+}]$ is the concentration of Fe(II) in the bulk of the solution. The proportionality constant k is defined by the Ilkovic equation and at $25^{o}C$ is equal to $607\ nD^{\frac{1}{2}}m^{2/3}t^{1/6}$. The concentration of Fe^{2+} at the surface of the electrode, $[Fe^{2+}]^{o}$ decreases with increasing current along the wave. When a constant

diffusion current, i_d, is attained, $[Fe^{2+}]^o$ has decreased to a value which is negligibly small compared to the concentration of Fe^{2+} in the body of the solution, $[Fe^{2+}]$. In other words, we have

$$i_d = k\,[Fe^{2+}] \tag{A-4}$$

By combining Eqs. 3 and 4 we obtain the following expression for $[Fe^{2+}]^o$ at any point on the wave.

$$[Fe^{2+}]^o = [Fe^{2+}] - \frac{i}{k} = \frac{i_d - i}{k}$$

or

$$[Fe^{2+}]^o = [Fe^{2+}]\cdot\frac{i_d - i}{i_d} \tag{A-5}$$

At the midpoint of the wave where $i = i_d/2$, $[Fe^{2+}]^o$ is equal to one-half of $[Fe^{2+}]$. The electrode potential, $E_{d.e.}$, in Eq. 2 is then equal to the half-wave potential, $E_{1/2}$. Therefore

$$E_{1/2} = E^o_{Fe^{2+}\rightarrow Fe(s)} + \frac{RT}{\alpha nF}\ln\frac{\gamma_{Fe^{2+}}[Fe^{2+}]}{2} \tag{A-6}$$

where $\gamma_{Fe^{2+}}$ is the activity coefficient of Fe^{2+}.

In the presence of catechol, the following complexes may form

$$Fe^{2+} + cat^{2-} = Fe(cat) \tag{A-7}$$

$$Fe^{2+} + 2cat^{2-} = Fe(cat)_2^{2-} \tag{A-8}$$

$$Fe^{2+} + 3cat^{2-} = Fe(cat)_3^{4-} \tag{A-9}$$

with formation constant of $Fe(cat)_j^{2-2j}$ defined as

$$\beta_j = \frac{(Fe(cat)_j^{2-2j})}{(Fe^{2+})(cat^{2-})^j} \tag{A-10}$$

The total iron concentration is given by

$$T_{Fe} = [Fe^{2+}] + [Fe(cat)] + [Fe(cat)_2^{2-}] + [Fe(cat)_3^{4-}] \tag{A-11}$$

or

$$T_{Fe} = [Fe^{2+}] + \frac{\beta_1[Fe^{2+}]\,\gamma_{Fe^{2+}}(cat^{2-})}{\gamma_{Fe(cat)}} + \frac{\beta_2[Fe^{2+}]\gamma_{Fe^{2+}}(cat^{2-})^2}{\gamma_{Fe(cat)_2^{2-}}}$$

$$+ \frac{\beta_3[Fe^{2+}]\,\gamma_{Fe^{2+}}(cat^{2-})^3}{\gamma_{Fe(cat)_3^{4-}}} \qquad \text{(A-12)}$$

$$\text{Define } \Sigma = \frac{1}{\gamma_{Fe^{2+}}} + \frac{\beta_1(cat^{2-})}{\gamma_{Fe(cat)}} + \frac{\beta_2(cat^{2-})^2}{\gamma_{Fe(cat)_2^{2-}}} + \frac{\beta_3(cat^{2-})^3}{\gamma_{Fe(cat)_3^{4-}}} \qquad \text{(A-13)}$$

$$\text{so} \qquad T_{Fe} = [Fe^{2+}]\Sigma\gamma_{Fe^{2+}} \qquad \text{(A-14)}$$

$$\text{or} \qquad [Fe^{2+}] = \frac{T_{Fe}}{\gamma_{Fe^{2+}}\Sigma} \qquad \text{(A-15)}$$

Substituting $[Fe^{2+}]$ expressed by Eq. 15 into Eq. 6, we obtain an expression for the half-wave potential in the presence of complexes, $E_{\frac{1}{2}}'$:

$$E_{\frac{1}{2}}' = E^{o}_{Fe^{2+}\rightarrow Fe(s)} + \frac{RT}{\alpha nF} \ln \frac{T_{Fe}}{2\Sigma} \qquad \text{(A-16)}$$

Substracting Eq. 6 from Eq. 14, recalling that when no complex formation occurs, $[Fe^{2+}] = T_{Fe}$, one obtains the shift in half-wave potential due to complex formation as:

$$\Delta E_{\frac{1}{2}} = \frac{-RT}{\alpha nF} \ln \gamma_{Fe^{2+}} \cdot \Sigma = \frac{-RT}{\alpha nF} \ln \gamma_{Fe^{2+}} \sum_{j=0}^{N} \frac{\beta_j(cat^{2-})^j}{\gamma_{Fe(cat)_j^{2-2j}}} \qquad \text{(A-17)}$$

If T_{cat} denotes the total concentration of catechol in solution we have

$$T_{cat} = [H_2cat] + [Hcat^-] + [cat^{2-}] + [Fe(cat)] + 2[Fe(cat)_2^{2-}] \quad \text{(A-18)}$$

Experimental conditions are chosen such that

$$T_{cat} >> T_{Fe} \quad \text{(A-19)}$$

hence

$$T_{cat} = [H_2cat] + [Hcat^-] + [cat^{2-}] \quad \text{(A-20)}$$

Giving β_p^H as the proton association constant of catechol

$$\beta_p^H = \frac{(H_pcat^{p-2})}{(cat^{2-})(H^+)^p} \quad \text{(A-21)}$$

we have

$$T_{cat} = \frac{\beta_2^H(cat^{2-})(H^+)^2}{\gamma_{H_2cat}} + \frac{\beta_1^H(cat^{2-})(H^+)}{\gamma_{Hcat^-}} + \frac{(cat^{2-})}{\gamma_{cat^{2-}}} \quad \text{(A-22)}$$

$$(cat^{2-}) = \frac{T_{cat}}{\frac{\beta_2^H(H^+)^2}{\gamma_{H_2cat}} + \frac{\beta_1^H(H^+)}{\gamma_{Hcat^-}} + \frac{1}{\gamma_{cat^{2-}}}} \quad \text{(A-23)}$$

$$= \frac{T_{cat}}{*_\Sigma} \quad \text{(A-24)}$$

where

$$*_\Sigma = \sum_{p=0}^{2} \frac{\beta_p^H(H^+)^p}{\gamma_{H_pcat^{p-2}}} \quad \text{(A-25)}$$

Substituting (cat^{2-}) expressed in Eq. 24 into Eq. 17 we have

$$\Delta E_{\frac{1}{2}} = \frac{-RT}{\alpha nF} \ln \gamma_{Fe^{2+}} \cdot \sum_{j=0}^{N} \frac{\beta_j}{\gamma_{Fe(cat)_j^{2-2j}}} \left(\frac{T_{cat}}{*_\Sigma}\right)^j \quad \text{(A-26)}$$

or

$$\exp\left\{\frac{-\Delta E_{\frac{1}{2}} \alpha nF}{RT}\right\} = \gamma_{Fe^{2+}} \cdot \sum_{j=0}^{N} \frac{\beta_j}{\gamma_{Fe(cat)_j^{2-2j}}} \left(\frac{T_{cat}}{*_\Sigma}\right)^j \quad \text{(A-27)}$$

If the stability constants are sufficiently different from one another there will be conditions under which only one complex, say the 1:1, the 1:2 or 1:3 complex, is the principle species in solution. If the 1:1 complex is the principal species, then Fe(cat) >> $Fe(cat)_2$ and Fe(cat) >> $Fe(cat)_3$. Under these conditions Eq. 25 reduces to

$$\exp\left\{\frac{-\Delta E_{\frac{1}{2}} \alpha nF}{RT}\right\} = \gamma_{Fe^{2+}} \left\{\frac{1}{\gamma_{Fe^{2+}}} + \frac{\beta_1 T_{cat}}{\gamma_{Fe(cat)} *_\Sigma}\right\}$$

$$= 1 + \frac{\gamma_{Fe^{2+}} \beta_1 T_{cat}}{\gamma_{Fe(cat)}} *_\Sigma^{-1} \quad \text{(A-28)}$$

Therefore, a graph of $\exp\left\{\frac{-\Delta E_{\frac{1}{2}} \alpha nF}{RT}\right\}$ vs. $*_\Sigma^{-1}$ will be a straight line with slope = $\beta_1 T_{cat} \gamma_{Fe^{2+}} / \gamma_{Fecat}$. The formation constant β_1 is thus obtainable from this slope.

Further rearrangement on Eq. 27 leads one to

$$*_\Sigma \left\{\exp\left(\frac{-\Delta E_{\frac{1}{2}} \alpha nF}{RT}\right) - 1\right\} = \frac{\gamma_{Fe^{2+}}}{\gamma_{Fecat}} \beta_1 T_{cat} +$$

$$\frac{\gamma_{Fe^{2+}}}{\gamma_{Fe(cat)_2^{2-}}} \beta_2 T_{cat}^2 (*_\Sigma)^{-1} \quad \text{(A-29)}$$

A plot of $*_\Sigma \left\{\exp\left(\frac{-\Delta E_{\frac{1}{2}} \alpha nF}{RT}\right) - 1\right\}$ against $*_\Sigma^{-1}$ will give a straight line

with slope = $\frac{\gamma_{Fe^{2+}}}{\gamma_{Fe(cat)^{2=}}} \beta_2 T_{cat}^2$. The formation constant β_2 is thus obtainable from this slope.